A reverse genetics and genomics approach to gene paralog function and disease: Myokymia and the juxtaparanode

Graphical abstract

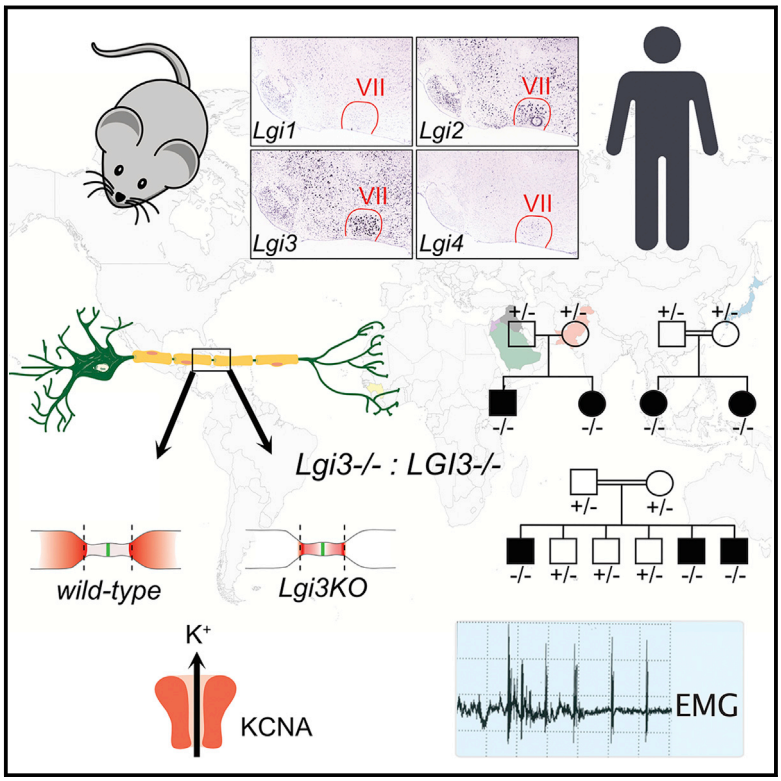

Authors

Dana Marafi, Nina Kozar, Ruizhi Duan, ..., James R. Lupski, Dies Meijer, Matias Wagner

Correspondence

jlupski@bcm.edu (J.R.L.), dies.meijer@ed.ac.uk (D.M.)

Through the power of human paralog gene studies, worldwide family-based genomics analyses, and mouse studies, we define a potentially-recognizable peripheral hyperexcitability syndrome in 16 individuals with bi-allelic *LGI3* variants and show that LGI3 co-localizes with juxta-paranodal voltage-gated potassium channels and its loss results in mis-localization of potassium channel complexes.

Marafi et al., 2022, The American Journal of Human Genetics *109*, 1713–1723
September 1, 2022 © 2022
https://doi.org/10.1016/j.ajhg.2022.07.006

A reverse genetics and genomics approach to gene paralog function and disease: Myokymia and the juxtaparanode

Dana Marafi,[1,2,36] Nina Kozar,[3,36] Ruizhi Duan,[2] Stephen Bradley,[3] Kenji Yokochi,[4,5] Fuad Al Mutairi,[6,7] Nebal Waill Saadi,[8,9] Sandra Whalen,[10] Theresa Brunet,[11,12] Urania Kotzaeridou,[13] Daniela Choukair,[14] Boris Keren,[15] Caroline Nava,[15] Mitsuhiro Kato,[16] Hiroshi Arai,[17] Tawfiq Froukh,[18] Eissa Ali Faqeih,[19] Ali M. AlAsmari,[19] Mohammed M. Saleh,[19] Filippo Pinto e Vairo,[20,21] Pavel N. Pichurin,[21] Eric W. Klee,[20,21,22] Christopher T. Schmitz,[23] Christopher M. Grochowski,[2] Tadahiro Mitani,[2,34] Isabella Herman,[2,24,25,35] Daniel G. Calame,[2,24,25] Jawid M. Fatih,[2] Haowei Du,[2] Zeynep Coban-Akdemir,[2,26] Davut Pehlivan,[2,24,25] Shalini N. Jhangiani,[27] Richard A. Gibbs,[2,27] Satoko Miyatake,[28,29] Naomichi Matsumoto,[28] Laura J. Wagstaff,[33] Jennifer E. Posey,[2] James R. Lupski,[2,25,27,30,37,*] Dies Meijer,[3,37,*] and Matias Wagner[31,32,37]

Summary

The leucine-rich glioma-inactivated (LGI) family consists of four highly conserved paralogous genes, *LGI1-4*, that are highly expressed in mammalian central and/or peripheral nervous systems. LGI1 antibodies are detected in subjects with autoimmune limbic encephalitis and peripheral nerve hyperexcitability syndromes (PNHSs) such as Isaacs and Morvan syndromes. Pathogenic variations of *LGI1* and *LGI4* are associated with neurological disorders as disease traits including familial temporal lobe epilepsy and neurogenic arthrogryposis multiplex congenita 1 with myelin defects, respectively. No human disease has been reported associated with either *LGI2* or *LGI3*. We implemented exome sequencing and family-based genomics to identify individuals with deleterious variants in *LGI3* and utilized GeneMatcher to connect practitioners and researchers worldwide to investigate the clinical and electrophysiological phenotype in affected subjects. We also generated *Lgi3*-null mice and performed peripheral nerve dissection and immunohistochemistry to examine the juxtaparanode LGI3 microarchitecture. As a result, we identified 16 individuals from eight unrelated families with loss-of-function (LoF) bi-allelic variants in *LGI3*. Deep phenotypic characterization showed *LGI3* LoF causes a potentially clinically recognizable PNHS trait characterized by global developmental delay, intellectual disability, distal deformities with diminished reflexes, visible facial myokymia, and distinctive electromyographic features suggestive of motor nerve instability. *Lgi3*-null mice showed reduced and mis-localized Kv1 channel complexes in myelinated peripheral axons. Our data demonstrate bi-allelic LoF variants in *LGI3* cause a clinically distinguishable disease trait of PNHS, most likely caused by disturbed Kv1 channel distribution in the absence of LGI3.

[1]Department of Pediatrics, Faculty of Medicine, Kuwait University, P.O. Box 24923, Safat 13110, Kuwait; [2]Department of Molecular and Human Genetics, Baylor College of Medicine, Houston, TX 77030, USA; [3]Centre for Discovery Brain Sciences, University of Edinburgh, Edinburgh, UK; [4]Department of Pediatrics, Toyohashi Municipal Hospital, Toyohashi, Aichi 441-8570, Japan; [5]Department of Pediatrics, Seirei Mikatahara General Hospital, Shizuoka 433-8558, Japan; [6]Genetics and Precision Medicine Department, King Abdullah Specialized Children's Hospital, King Abdulaziz Medical City, Ministry of National Guard Health Affairs, P.O. Box 22490, Riyadh 11426, Kingdom of Saudi Arabia; [7]King Abdullah International Research Center, King Saud Bin Abdulaziz University for Health Sciences, Ministry of National Guard Health Affairs, Riyadh, Kingdom of Saudi Arabia; [8]College of Medicine, University of Baghdad, Baghdad 10001, Iraq; [9]Children Welfare Teaching Hospital, Medical City Complex, Baghdad 10001, Iraq; [10]UF de Génétique Clinique et Centre de Reference Anomalies du Développement et Syndromes Malformatifs, APHP, Sorbonne Université, Hôpital Trousseau, 75005 Paris, France; [11]Institute of Human Genetics, Faculty of Medicine, Technical University Munich, Munich, Germany; [12]Institute of Human Genetics, Helmholtz Zentrum München, Neuherberg, Germany; [13]Division of Child Neurology and Inherited Metabolic Diseases, Centre for Pediatrics and Adolescent Medicine, University Hospital Heidelberg, Heidelberg, Germany; [14]Division of Pediatric Endocrinology, Centre for Pediatrics and Adolescent Medicine, University Hospital Heidelberg, Heidelberg, Germany; [15]Département de Génétique, Hôpital Pitié-Salpêtrière, Assistance Publique - Hôpitaux de Paris, Paris 75013, France; [16]Department of Pediatrics, Showa University School of Medicine, Tokyo 142-8666, Japan; [17]Department of Pediatric Neurology, Bobath Memorial Hospital, Osaka 536-0023, Japan; [18]Department of Biotechnology and Genetic Engineering, Philadelphia University, Amman, Jordan; [19]Section of Medical Genetics, King Fahad Medical City, Children's Specialist Hospital, Riyadh, Saudi Arabia; [20]Center for Individualized Medicine, Mayo Clinic, Rochester, MN, USA; [21]Department of Clinical Genomics, Mayo Clinic, Rochester, MN, USA; [22]Department of Quantitative Health Sciences, Mayo Clinic, Rochester, MN, USA; [23]Department of Biochemistry and Molecular Biology, Mayo Clinic, Rochester, MN, USA; [24]Section of Pediatric Neurology and Developmental Neuroscience, Department of Pediatrics, Baylor College of Medicine, Houston, TX 77030, USA; [25]Texas Children's Hospital, Houston, TX 77030, USA; [26]Human Genetics Center, Department of Epidemiology, Human Genetics, and Environmental Sciences, School of Public Health, The University of Texas Health Science Center at Houston, Houston, TX, USA; [27]Human Genome Sequencing Center, Baylor College of Medicine, Houston, TX 77030, USA; [28]Department of Human Genetics, Yokohama City University Graduate School of Medicine, Yokohama, Kanagawa 236-0004, Japan; [29]Clinical Genetics Department, Yokohama City University Hospital, Yokohama, Kanagawa 236-0004, Japan; [30]Department of Pediatrics, Baylor College of Medicine, Houston, TX 77030, USA; [31]Institute for Neurogenomics, Helmholtz Zentrum München, Neuherberg, Germany; [32]Institute of Human Genetics, Technical University Munich, Munich, Germany; [33]Centre for Regenerative Medicine, Institute for Regeneration and Repair, University of Edinburgh, Edinburgh, UK
[34]Present address: Department of Pediatrics, Jichi Medical University, 3311-1 Yakushiji, Shimotsuke, Tochigi, 329-0498, Japan
[35]Present address: Department of Neurosciences, Boys Town National Research Hospital, Boys Town, NE 68010, USA
[36]These authors contributed equally
[37]These authors contributed equally
*Correspondence: jlupski@bcm.edu (J.R.L.), dies.meijer@ed.ac.uk (D.M.)
https://doi.org/10.1016/j.ajhg.2022.07.006.

The leucine-rich glioma-inactivated (LGI) family consists of four highly homologous proteins, LGI1-4, composed of two repeat domains: N-terminal cysteine-flanked leucine-rich repeats (LRRs) and C-terminal epitempin (EPTP) repeats.[1,2] These repeats exhibit 60%–70% similarity in their amino acid sequence and highly similar domain structures, categorizing LGI1-4 within the large LRR and EPTP superfamilies.[2]

Members of the EPTP superfamily have been proposed as candidates for epilepsy and neurological disorders.[2] *LGI1-4* paralogues are highly expressed in the central and/or peripheral nervous system (CNS and PNS, respectively).[3,4] LGI3 is widely expressed in the mammalian brain,[3] where it co-localizes and interacts with endocytosis-associated proteins and SYNTAXIN-1, potentially regulating neuronal endocytosis and exocytosis.[5,6] *LGI3* expression increases dramatically during postnatal brain development, suggesting a role in neuronal differentiation, maturation, synaptogenesis, and plasticity.[7] *LGI3* is highly expressed in sensory and motor neurons in the PNS and induces neurite outgrowth in dorsal root ganglia explants.[4,8,9]

No known disease associations exist for *LGI3* (MIM: 608302), but its paralogues *LGI1* (MIM: 604619) and *LGI4* (MIM: 608303) associate with neurological disease traits: familial temporal lobe epilepsy (FTLE [MIM: 600512]) and neurogenic arthrogryposis multiplex congenita 1, with myelin defects (AMC1 [MIM: 617468]), respectively.[10–13] Antibodies against LGI1 can be found in acquired autoimmune limbic encephalitis and peripheral nerve hyperexcitability syndromes (PNHSs).[14,15]

PNHSs are a rare group of neurological disorders characterized by clinical and electrodiagnostic evidence for instability of neurotransmission in lower motor neurons or peripheral motor nerves resulting in spontaneous discharges, such as fasciculations, myokymia, neuromyotonia, and overactivity of the muscle groups, leading to muscle stiffening, cramps, and gait impairment.[14] Occasionally, CNS features such as agitation, memory loss, ataxia, dysarthria, seizures, autonomic dysfunction, dystonia, and/or dyskinesia are observed.[14,16–18] The majority of PNHSs are acquired immune-mediated disorders, including Isaacs syndrome [MIM: 160120], Morvan syndrome, and cramp-fasciculation syndrome.[14]

Evidence for peripheral nerve hyperexcitability is observed in several genetic syndromes, the "genetic PNHSs," such as *KCNA1*-related episodic ataxia type 1 (EA1)/myokymia syndrome (MIM: 160120), *KCNQ2*-related benign familial neonatal epilepsy type 1 and/or myokymia (MIM: 121200), *HINT1*-related neuromyotonia and axonal neuropathy (MIM: 137200), *ADCY5*-related familial dyskinesia with facial myokymia (MIM: 606703), and *PNKD*-related paroxysmal non-kinesigenic dyskinesia 1 (MIM: 118800).

We describe a genetic PNHS due to bi-allelic *LGI3* LoF in 16 subjects from eight unrelated families. Prominent clinical features include global developmental delay (GDD), intellectual disability (ID), facial myokymia, distal deformities, and hyporeflexia/areflexia demonstrating both CNS and PNS dysfunction. Our data in mice and humans suggest a plausible model to explain electrodiagnostic myokymia and the appearance of observable facial myokymia.

Legal guardians of affected individuals provided written informed consent for clinical data sharing, collection and storage of biological samples, experimental analyses, and publication of relevant findings as well as images and videos. The study was performed in agreement with the Declaration of Helsinki and was approved by the relevant institutional ethics committees from participating centers that connected through GeneMatcher.[19] Individual case reports can be found in the supplemental notes. Family 4 was previously included in a gene discovery cohort.[20] Exome sequencing (ES) was implemented with genomic DNA extracted from leukocytes. Sanger di-deoxynucleotide sequencing was performed in all available family members and have validating variant alleles and confirmed their segregation in accordance with Mendelian expectations (supplemental information). We used unphased ES data in families 1, 5, and 6 to determine absence of heterozygosity (AOH) of genomic intervals and infer runs of homozygosity (ROH) representing haplotypes "homozygosed" via identity by descent (IBD) versus identity by state (IBS) and to calculate the estimated coefficient of inbreeding, FROH, for fraction of genome shared (supplemental information). We used ExomeDepth, a tool utilizing read depth from ES data as a surrogate measure of copy-number variants (CNVs), to detect the homozygous multi-exonic intragenic deletion in *LGI3* in family 1.[21] Characterization of the exonic CNV event, breakpoint junctions, and inference of mutational mechanisms is detailed in the supplemental information.

Families originated from multiple countries and diverse ethnic backgrounds (Figure 1A and Table 1). All families reported a history of consanguinity with first-degree-cousin marriage except for two families (family 5A and family 7). Family 5A's parents however were descendants of the same large tribe. The estimated inbreeding co-efficient FROH of their affected children (family 5A, II-1 and II-2) was 0.04 and 0.022, respectively, approaching that of a second-degree-cousin marriage ($F = 0.03125$).

All *LGI3* variants found in these families are listed in Table 1. Identified variants have been deposited to ClinVar (ClinVar: SUB11712385). Alleles include five predicted LoF variants (three frameshift, one nonsense, and one multi-exonic deletion) and two missense variant alleles (Table 1 and Figures 1C and S1; [GenBank: NM_139278.4]). The two intronic +1/−1 variants (8: 22011480, c.494+1G>C and 8: 22006491, c.830 1G>A) are located at a canonical splice site that most likely causes aberrant splicing (SpliceAI highest confidence score (0.99–1.00) on both variants).[22] How such putative splicing defects affect LGI3 protein expression remains to be determined.

The missense variant p.Leu141His localizes to the LRR domain whilst the missense variant p.Asp331Asn

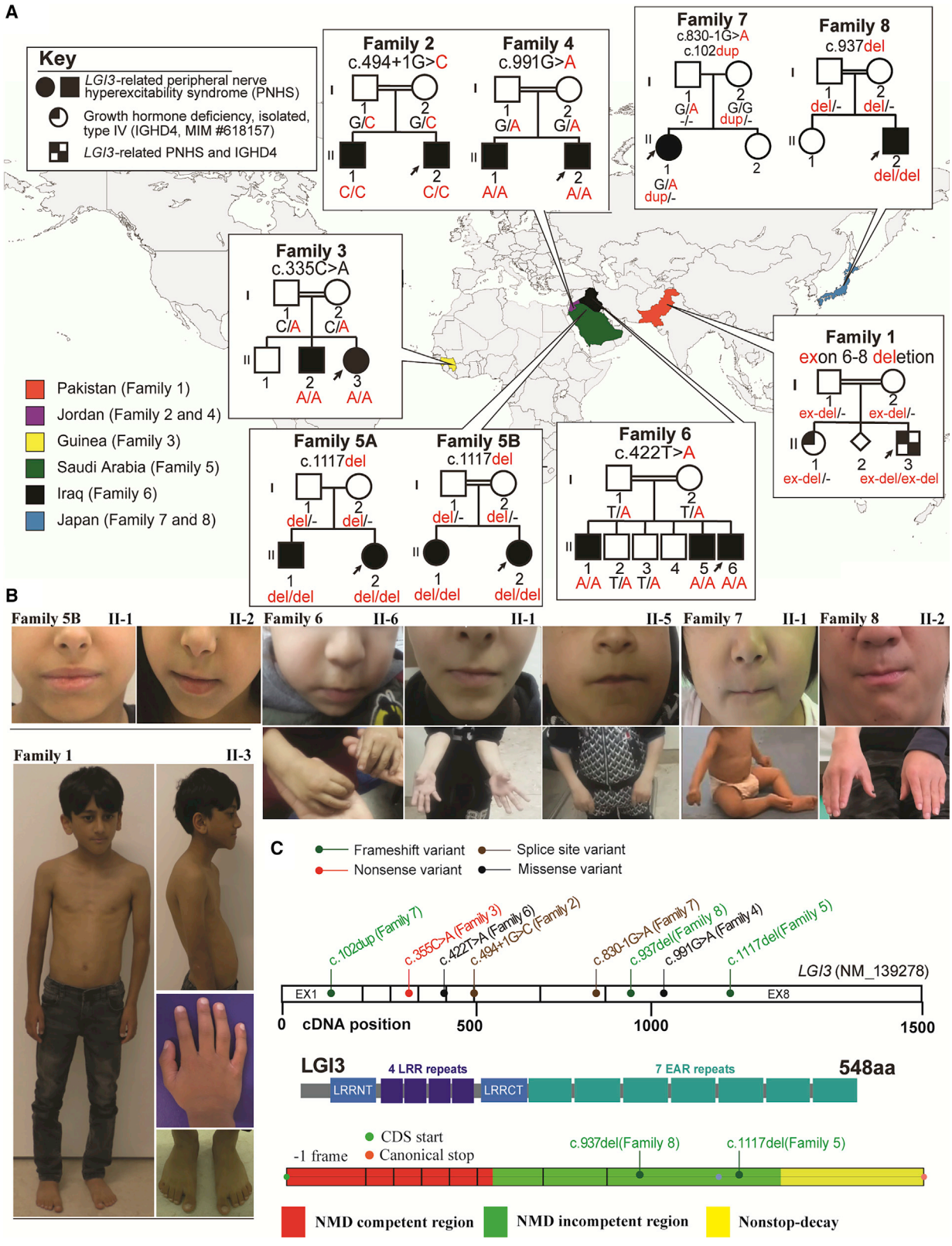

Figure 1. Pedigrees, photographs, and variants' location in the eight families with bi-allelic variants in *LGI3*

(A) A world map showing countries of origin of each family in the study along with their pedigree. The genotype of the variant can be found under each individual in the pedigree.

(B) All available clinical photos of affected individuals with *LGI3*-related disorder in this study are displayed. Note the small mouth (except for family 5B, II-1 and II-2) and distal deformities in the fingers in the affected individuals. Individual II-3 (family 1) also has short stature, thin build, and genu valgum, syndactyly, camptodactyly, and kypholordosis.

(C) A schematic of *LGI3* with the location of the variants across the gene shown. Below the gene structure is the LGI3 protein structure with its different domains including the LRR and EAR repeats.

Table 1. Summary of *LGI3* variant alleles in the eight unrelated families

Family	Country of origin	Consanguinity by history	Position (GRCh37\ hg19)	Nucleotide (protein) (GenBank: NM_139278.4)	dbSNP ref.	Zygosity	Allele count/ zygosity (gnomAD)	CADD score (PHRED)	Conservation, 100 vert, cons. (phyloP100 wayAll)	AOH (around *LGI3*/ total)
Family 1	Pakistan	yes (1° cousins)	del exons 6-8		N/A	hmz	N/A	N/A	N/A	40 Mb/ 330 Mb
Family 2	Jordan	yes (1° cousins)	chr8: 22011480; C>G	c.494+1G>C	rs1827450545	hmz	0 htz–0 hmz	33	7.14961	N/A
Family 3	Guinea	yes (1° cousins)	chr8: 22012088; G>T	c.335C>A (p.Ser112*)	rs769376680	hmz	2 htz–0 hmz	41	4.93405	N/A
Family 4	Jordan	yes (1° cousins)	chr8: 22006329; C>T	c.991G>A; (p.Asp331Asn)	rs1050199719	hmz	1 htz–0 hmz	26.1	4.43004	N/A
Family 5A	Saudi Arabia	no	chr8: 22006203; delA	c.1117del (p.Trp373 Glyfs*18)	N/A	hmz	0 htz–0 hmz	N/A	9.27922	15/265–300 Mb
Family 5B		yes (1° cousins)								2 Mb/ 107–237 Mb
Family 6	Iraq	yes (1° cousins)	chr8: 22011655; A>T	c.422T>A (p.Leu141His)	N/A	hmz	0 htz–0 hmz	33	9.0998	23–28 Mb/ 604–647 Mb
Family 7	Japan	no	chr8: 22006491; C>T (pat)	c.830−1G>A	N/A	comp htz	0 htz–0 hmz	33	7.07505	N/A
			chr8: 22013954; dupG (mat)	c.102dup (p.Lys35G lnfs*86)	Rs749644081		0 htz–0 hmz	N/A	0.132937	N/A
Family 8	Japan	yes (1° cousins)	chr8: 22006383; delT	c.937del (p.Thr313 Argfs*20)	N/A	hmz	1 htz–0 hmz	N/A	0.756417	N/A

Abbreviations: AOH, absence of heterozygosity; CADD, combined annotation-dependent depletion; comp htz, compound heterozygous; hmz, homozygous; htz, heterozygous; mat, maternal inherited; N/A, not available; pat, paternal inherited; ref., reference.

(encoded by c.991G>A) localizes to the EPTP domain. The mutant encoding p.Leu141His variant (c.422T>A) is located 1 bp from the exon-intron junction but is predicted not to affect mRNA splicing (SpliceAI score of 0.00–0.09).[22] Both missense mutations are predicted to be damaging, and we show that indeed the mutant proteins accumulate in the endoplasmic reticulum (ER) and are secreted at severely reduced levels (Figures S1B–S1E). Thus, these mutations represent probable functional-null alleles of *LGI3*. However, it is likely that the clinical phenotype of members of families 4 and 6 is further impacted by ER stress, as production of these mutant proteins results in strong ER accumulation and upregulation of chaperone proteins (Figure S1E–E1).

The deleterious variants in *LGI3* were homozygous and conformed with expected autosomal recessive (AR) trait inheritance in all families except for family 7 with no reported consanguinity or tribal marriage in which the variants were compound heterozygous.

Interestingly, the two branches of family 5 (5A and 5B) were not known to be related but were from the same geographic region and carried the same variant allele that may represent a clan genomics-derived founder allele.[23] Further exploration of extended pedigrees revealed a shared ancestor, and the variant allele was identified within an overlapping AOH block of 1.9 Mb with a total AOH of 107–137 Mb by AOH haplotype analysis of affected children (Figure S2). Note the *LGI3* embedded AOH block of 15 Mb for family 5B with a total AOH of 265–300 Mb (Figure S2). Two subjects carried a second molecular aberration, including chr16q13.11 microduplication of unknown significance (family 7; individual II-1) and pathogenic homozygous variant in *GHRHR* (c.214G>T [p.Glu72*] [GenBank: NM_000823.3]) (family 1, II-3) causing AR isolated growth hormone deficiency type IV (IGHD4 [MIM: 618157]); thus, the multi-locus pathogenic variation in this proband may result genetically by distributive ROH.

A homozygous intragenic deletion involving exons 6 to 8 of *LGI3*, which has eight coding exons, was identified in the proband from family 1 (Figure 2A). Nucleotide-level resolution of the breakpoint junction was obtained and confirmed a homozygous deletion allele (~1.5 kb band) in proband genomic DNA (gDNA), suggesting genomic deletion size of ~6.9 kb; both parents and the unaffected sister were heterozygous carriers of the exonic deletion. In contrast, only the wild-type (WT) allele (~8.4 kb band) was observed in the gDNA control (Figure 2B).

Eight possible CNV-*Alu* pairs were predicted with an AAMR genomic instability risk score of 0.469 for MIM

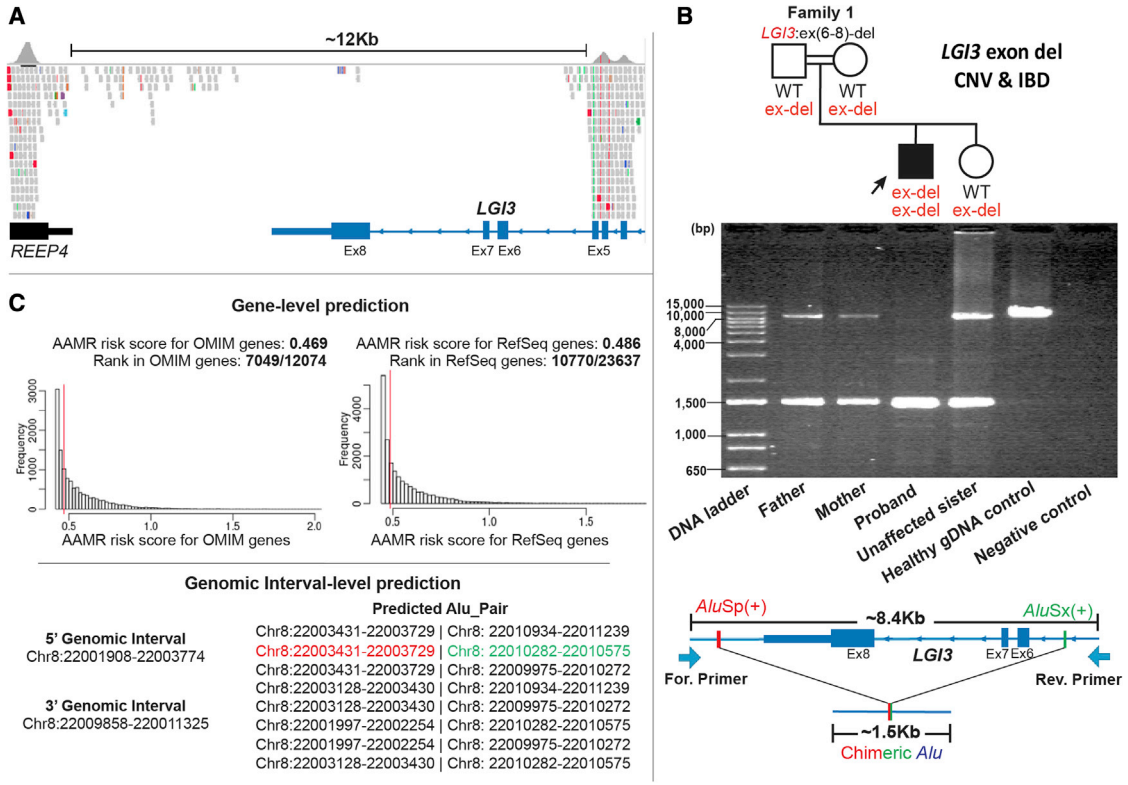

Figure 2. The genomic architecture of the multi-exonic intragenic deletion of *LGI3* in amily 1 derived from an *Alu/Alu*-mediated genomic rearrangement (AAMR)

(A) A screenshot of the proband's exome sequencing data (integrated genomic view [IGV]) showing an approximately 12 kb homozygous intragenic deletion involving exons 6–8 of the exon *LGI3*.

(B) A pedigree of the family 1 followed by the 1% agarose gel electrophoresis of PCR products generated using a primer flanking exon 6–8 in *LGI3* and positioned 8.4 kb apart. From left to right: parents with two bands of ~1.5 kb and ~8.4 kb representing the two alleles at this locus and consistent with the expected sizes for one deleted and one wild-type (WT) non-deleted allele (WT = reference haploid genome); proband with a PCR band of ~1.5 kb consistent with a single deleted allele; unaffected sister with two bands, heterozygous alleles, like parental alleles; healthy gDNA control with one WT non-deleted allele (~8.4 kb band); and negative control (no template). The schematic below the gel shows the genomic profile of *Alu*Sp/*Alu*Sx-pair-mediated rearrangement. The long-range PCR primer pair was designed to produce an amplicon size of ~8.4 kb for WT non-deleted allele and ~1.5 kb for deleted allele resulting from AAMR with formation of a recombinant or chimeric *Alu*.

(C) A screenshot from AluAluCNVPredictor shows gene-level prediction including AAMR risk score of *LGI3* in MIM genes and RefSeq genes. A gene with a risk score higher than 0.6 is considered "at increased relative risk" for genomic instability and susceptibility to AAMR. Genomic interval-level prediction shows eight possible CNV-*Alu* pairs intersecting the given genomic intervals. The specific *Alu*Sp/*Alu*Sx pair that was implicated by experimental data in generating the intragenic deletion in this family is marked with colored font.

genes and 0.486 for RefSeq genes; the latter references haploid human genome computationally annotated genes for *LGI3* (Figure 2C). Examination of the haploid human reference genome showed multiple directly oriented *Alu* elements flanking the deletion region, suggesting potential susceptibility to AAMR (Figure S3A). Sanger sequencing across the breakpoint junction in the deleted allele showed a chimeric, or recombinant, *Alu* element yielded from *Alu*Sp/*Alu*Sx recombination, with 65 bp microhomology at the apparent recombinant joint (Figure S3B) consistent with AAMR's generating the new mutation haplotype in the clan.

Table 2 summarizes the developmental and neurological features of the 16 individuals from eight unrelated families with deleterious bi-allelic *LGI3* variants (further detailed in supplemental notes and Tables S1 and S2). All affected subjects had mild to moderate GDD (16/16), ID (13/13). Prominent neurological features included distal limb deformities (14/16); areflexia or hyporeflexia (10/16); tone abnormalities (7/13) including lower limb hypotonia in three subjects (one also with truncal hypotonia) and peripheral hypertonia/stiffness in five; and near-continuous facial myokymia (7/16) (Video S1) associated with a small mouth with restricted opening (6/16). The facial myokymia was noted as early as 3 months of age (family 6). Distal deformities included knee, hip, and ankle contractures (4/14); contractures/deformities of fingers and feet (6/14); and other uncharacterized deformities (4/14).

Less common features included umbilical or diaphragmatic hernias (4/16), gait abnormality (5/16), neurobehavioral traits including autism spectrum disorder (5/16) or attention deficit hyperactivity disorder (4/16), tongue

Table 2. Developmental and neurological features in the 16 affected individuals with bi-allelic deleterious variants in *LGI3*

	Developmental characteristics				Neurological features						
Individuals	Age at last exam	Sex	GDD	ID	Areflexia/ hyporeflexia	Distal deformities	Facial myokymia	Small mouth with restricted opening	Tongue fasciculations	Abnormal NCS	Myokymia or fasciculations on EMG
Family 1, II-3	7 years	M	+	N/A	+	+	–	–	–	–	N/A
Family 2, II-1	9 years	M	+	N/A	+	+	–	–	–	N/A	+
II-2	6 years	M	+	N/A	+	+	–	–	–	+	+
Family 3, II-2	7 years	M	+	+	+	+	+	+	+	N/A	–
II-3	4 years 7 months	F	+	+	+	+	+	+	+	N/A	+
Family 4, II-1	22 years	M	+	+ (mild)	–	–	–	–	–	N/A	N/A
II-2	20 years	M	+	+ (mild)	–	–	–	–	–	N/A	N/A
Family 5A, II-1	11 years	M	+	+ (mild)	–	+	–	–	–	–	–
II-2	9 years	F	+	+ (mild)	–	+	–	–	–	–	–
Family 5B, II-1	13 years	F	+	+ (mild)	–	+	–	–	–	N/A	N/A
II-2	9 years	F	+	+ (mild)	–	+	–	–	–	N/A	N/A
Family 6, II-1	13 years	M	+	+ (moderate)	+	+	+	+	–	–	N/A
II-5	6 years	M	+	+ (mild)	+	+	+	+	–	–	+
II-6	3 years	M	+	+ (mild)	+	+	+	+	–	N/A	N/A
Family 7, II-1	12 years 10 months	F	+	+ (moderate)	+	+	+	–	–	–	+
Family 8, II-2	13 years	M	+	+ (moderate)	+	+	+	+	+	N/A	N/A
Total	n/a	n/a	16/ 16	13/13	10/16	14/16	7/16	6/16	3/16	1/7	5/8

Abbreviations: EMG, electromyography; F, female; GDD, global developmental delay; ID, intellectual disability; M, male; N/A, not available; n/a, not applicable; NCS, nerve conduction study.
Through the power of human paralog gene studies, worldwide family-based genomics analyses, and mouse studies, we define a potentially recognizable peripheral hyperexcitability syndrome in 16 individuals with bi-allelic *LGI3* variants and show that LGI3 co-localizes with juxtaparanodal voltage-gated potassium channels and its loss results in mis-localization of potassium channel complexes.

fasciculations (3/16), and seizures (2/16). Other rarely observed features—seen only in one subject each—include severe progressive microcephaly (Z score −5 SD), failure to thrive (FTT; weight at −4 SD), short stature (height at −4 SD), growth hormone (GH) deficiency, kyphosis (in family 1, II-3 with IGHD4), bilateral hip dysplasia, *pectus carinatum*, anxiety, eczema, celiac disease, hypokinesia, and ataxia.

Nerve conduction studies (NCSs) were normal in six subjects (6/7) while one subject (1/7) (family 2, II-2) at age 6 years had an abnormal NCS consistent with an axonal neuropathy (supplemental information, Table S2). Myokymic discharges or fasciculations were characteristically observed in the majority (5/8) of those who underwent an EMG study (Figure S4); the discharges were not related to age or variant type. Muscle biopsy was performed in two siblings (family 2) with non-specific findings of increased citrate synthase activity without deficiency in respiratory chain enzymes in the first child and slight denervation atrophy with type 1 fiber "smallness" in some fascicles in the sibling. Brain MRI was normal in most subjects (6/8) and abnormal in two subjects. One subject, with a second molecular diagnosis causing GH deficiency, showed a small hypophysis, whereas the other showed mild frontal hypoplasia. Four subjects underwent routine EEG study, which revealed occasional epileptiform activity in two subjects, one of which has seizures (family 4, II-1).

The myokymic discharges and fasciculations observed in a subset of individuals could result from perturbations to

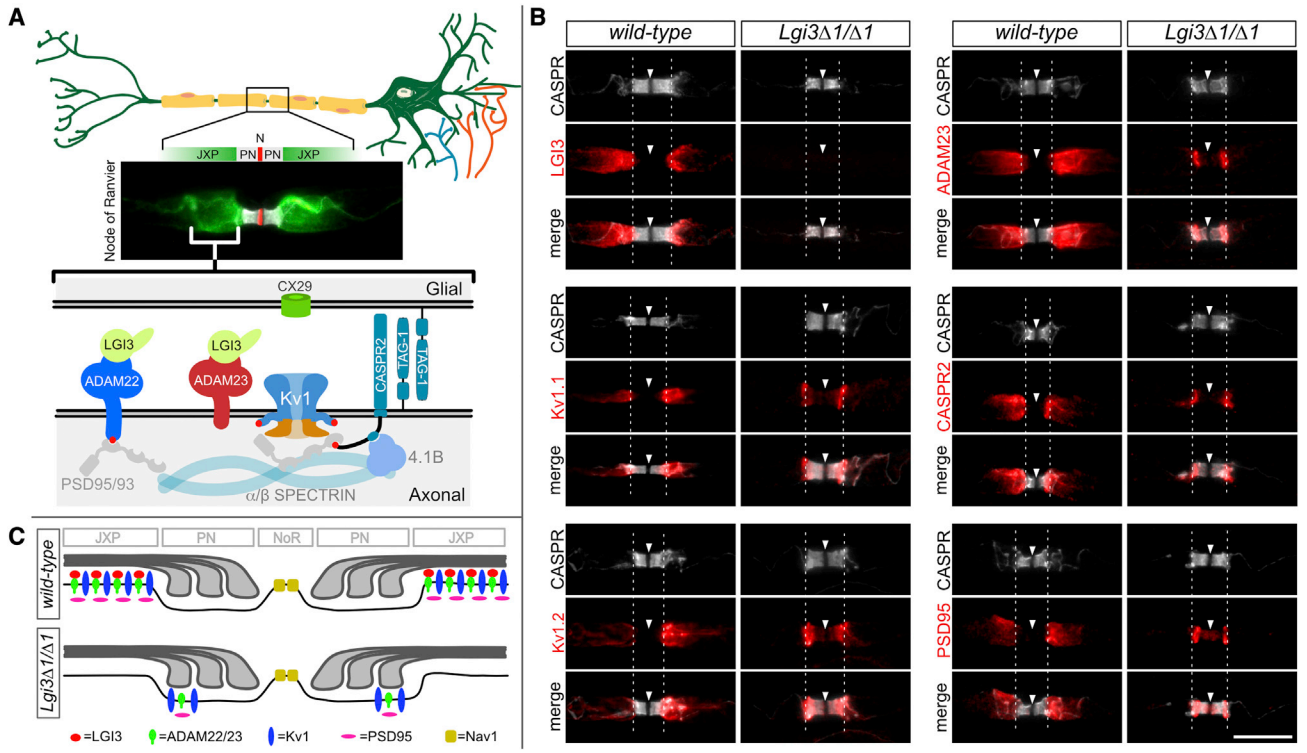

Figure 3. A schematic illustration of the myelinated peripheral nerves, the microanatomy of the nodes of Ranvier

(A) Saltatory conduction in myelinated axons depends on the sequestration of voltage-gated ion channels to the node of Ranvier, the narrow gaps between adjacent myelin sheets. The immune fluorescence image shows the distribution of Kv1 voltage-gated potassium channels (green) under the myelin sheet, in what is referred to as the juxtaparanodal membrane, next to the paranodal junctions (PN in gray) that separate them from the voltage-gated sodium channels Nav1 in the nodal membrane (N in red). At the bottom is a schematic illustration of the juxtaparanodal region highlighting some of the proteins that are highly expressed here. LGI3 binds ADAM23 and/or ADAM22 in the juxtaparanodal membrane. Note that Kv1.1, CASPR2 (CNTNAP2), and TAG-1 (CNTN2) have been implicated in autoimmune peripheral nerve hyperactivity syndrome (PNHS). Additionally, *CASPR2* (MIM: 610042) and *ADAM22* (MIM: 617933) have been implicated in neurodevelopmental disorders and epilepsies and *LGI4* and *CASPR* (also known as *CNTNAP1*) (MIM: 616286), a component of the paranodal junctions, in neurogenic arthrogryposes.

(B) Loss of LGI3 results in reduced and mis-localized Kv1 channel complex in myelinated axons. Representative images of nodes of Ranvier in sciatic nerve axons of 8 week-old WT and *Lgi3* $^{\Delta 1/\Delta 1}$ mice immunolabelled with antibodies against the paranodal protein CASPR (CNTNAP1) (grey) and members of the JXP: LGI3, Kv1.1, Kv1.2, ADAM23, CASPR2 (CNTNAP2), and PSD95 (DLG4) (red). Arrowheads (node) and dashed lines (PN/JXP border) highlight the localization of JXP proteins in the paranode of mutant mice compared to their JXP expression in WT controls. Scale bar: 10 μm.

(C) Graphical representation of the distribution of JXP Kv1 complexes in the presence and absence of LGI3.

the myelinated axons of the facial nerve. We therefore explored whether the LGI3 is present in the myelinated axons of the mouse PNS and what consequence deletion of *Lgi3* has. LGI3 is found at high levels in PNS sensory and motor neurons (Allen Mouse Brain Atlas: https://mouse.brain-map.org/).[4] Within peripheral myelinated axons, LGI3 is highly expressed at the juxtaparanodal membrane, co-localizing with the voltage-gated potassium channels Kv1.1 (KCNA1) and Kv1.2 (KCNA2), associated proteins CASPR2 (CNTNAP2) and PSD95 (DLG4), and the LGI-binding proteins ADAM23 and ADAM22 (Figure 3A and 3B). To assess how loss of LGI3 impacts this organization, we generated homozygous *Lgi3*-null mice (*Lgi3*$^{\Delta 1/\Delta 1}$, Figure S6). *Lgi3* mutant mice are fertile, have a normal lifespan, and do not show obvious behavioral abnormalities. We found that the homozygous deletion of *Lgi3* resulted in strongly reduced expression and mis-localization of Kv1 channel complexes that infringe on the paranodal domain (Figures 3B and 3C). This mis-localization of Kv1 channel complexes is further exacerbated following nerve injury, as Kv1 complexes are confined to the paranodal domain in remyelinated axons (Figure S5). It is speculated that these reduced and mis-localized Kv1 complexes affect the electrophysiological characteristics of the myelinated axons and contribute to the axonal hyperexcitability that underpins the observed myokymia in PNHS subjects homozygous for *LGI3* LoF alleles.

The majority of the subjects had neuropathic features such as distal contractures/deformities (14/16) and diminished reflexes (10/16) despite normal NCSs (6/7). Depressed reflexes have been observed in autoimmune PNHSs.[24] Interestingly, motor and sensory NCSs are often normal in Isaacs syndrome, an autoimmune PNHS, except for after-discharges best observed on repetitive nerve stimulation, which were not performed in any of our

subjects.[24] Additionally, nearly half of our subjects (7/16) had characteristic clinically visible facial myokymia, and the majority of those who underwent EMG (5/8) had findings suggestive of motor nerve hyper-excitability such as myokymia and/or fasciculations. The reason for normal NCS despite the presence of neuropathic features remains to be explored.

Myo-kymia, Greek for "muscle waves," was first reported in the late 1800s independently by two German clinicians, Kny and Schultze.[14,25,26] Facial myokymia, a distinct neurological phenomenon and an exceedingly rare form of myokymia, was described later in 1902 by Bernhardt as "continuous undulant quivering fasciculation of the muscles of the face".[27] In a majority of cases, the myokymia occurs abruptly because of an acquired etiology, specifically pontine glioma and multiple sclerosis, although idiopathic cases have been described.[18,27–29] Myokymia is thought to represent abnormal firing of the motor neuron or peripheral motor nerves.[16] The pathology in facial myokymia is speculated intramedullary in the brainstem and close to the facial nucleus.[27,29] Many subjects also had narrowing of the palpebral fissures, updrawn angle of the mouth, and similar to our subjects, pursing of the lips consistent with the wide involvement of facial musculature as a potential underlying basis of the facial dysmorphology gestalt.[27,29]

Facial myokymia has also been observed in *ADCY5*-related disorder (MIM: 606703) in association with chorea/dyskinesia disorder and in a subject with dominant-negative heterozygous *KCNQ2* mutation with distal contractures and febrile seizures but, in contrast to our subjects, without GDD/ID.[16,18] The visible myokymia in *LGI3*-related disorder is restricted to the face (peri-orbital and peri-oral). Few subjects also had tongue fasciculations and electromyographic myokymia and fasciculations suggesting the involvement of other cranial and peripheral nerves (Table 2 and Table S1). Myokymia, neuromyotonia, and fasciculations can also occur in other genetic PNHSs, such as *HINT1*-, *KCNA1*-, and *PNKD*-related disorders (MIM: 137200, 160120, and 118800, respectively).[30]

The overlap between acquired immune-related and genetic (inherited) disorders is an evolving concept, and exploring myokymia in both acquired and inherited disease can reciprocally inform the mechanism and pathogenesis of both.[31,32] The implication of voltage-gated potassium channels (VGKCs) in both autoimmune and genetic PNHSs is a salient example. Autoimmune PNHSs are occasionally paraneoplastic in origin, and antibodies against VGKC complex are often detected.[14,33] In parallel, mutations in *KCNA1* and *KCNQ2* encoding juxtaparanodal and nodal VGKCs (Kv1.1 and Kv7.2, respectively) associate with myokymia.[17,18] VGKCs dampen neuronal excitability by determining resting action potential, setting threshold for excitation, controlling firing frequency, and promoting repolarization after action potential.[34,35] Suppression of outward VGKCs' current and induced repetitive nerve firing in dorsal root ganglia is observed in subjects with Isaacs syndrome.[36,37]

Notably, anti-VGKC complex antibodies are not solely directed towards VGKCs but often target associated complex-forming proteins such as CASPR2 and CONTACTIN-2 (CNTN2, also called TAG-1), as well as LGI1, although the majority of antigen targets remain unknown (Figure 3).[33] It is thus not surprising to see that impairment of VGKC in the PNS and its interactomes are heavily implicated in PNHSs. Indeed, we demonstrate that loss of LGI3 in mice affects VGKCs and results in strongly reduced and mis-localized expression of Kv1 protein complexes at the juxtaparanodal domain of the node of Ranvier thus likely contributing to the PNHS phenotype (Figure 3). How other genetic PNHS-associated proteins, such as ADCY5 and PNKD, potentially interact with VGKCs remains to be explored. We propose that identifying and describing genetic PNHSs, such as *LGI3*-related disorder, can inform the neurobiology of axonal transmission and illuminate the pathophysiology of immune-related PNHS and potentially define new antigen targets.

Genetic PNHSs have an overlapping organismal phenotype, yet each has unique features in sync with the protein's function and its anatomical and temporal expression. The paroxysmal episodes of ataxia and dysarthria, painful contractures, and myokymia in *KCNA1*-related EA1 are compatible with the Kv1.1 expression in the cerebellum and peripheral nerves.[17,35] *ADCY5* is highly expressed in the striatum correlating with the associated movement disorder phenotype.[16] Furthermore, the Kv7.2 (KCNQ2) peak brain expression at birth and its expression at the nodes of Ranvier and axon initial segment is consistent with the *KCNQ2*-related neonatal seizures and myokymia phenotype.[34,38] Similarly, the CNS and PNS features of this *LGI3*-related disorder align with LGI3's widespread cortical and peripheral nerve expression and role in brain development, neurite growth, and peripheral nerve biology.[7,9,39,40] Interestingly, *LGI3* expression is detected most strongly in the facial nerve nucleus concurring with proposed pathophysiology of facial myokymia.[27,29]

Severe progressive microcephaly (PM), short stature, FTT, GH deficiency, and small hypophysis (as revealed by neuroimaging) were observed in only one individual in this study who also carried a second molecular diagnosis: a *GHRHR* homozygous variant causing IGHD4 (MIM: 618157) that explains the severe growth failure but not the PM. Multi-locus pathogenic variation (MPV) in which variations at two or more genetic loci lead to a blended phenotype accounts for 5% of simplex cases with molecular diagnoses established by clinical exomes and up to 29% of neurodevelopmental disorder (NDD) cases from consanguineous families with increased FROH.[41–43] The individual's total genomic AOH is 330 Mb and consistent with a distributive ROH, raising the possibility for a third contributing locus to explain the PM. Interestingly, one-third of the subjects with NDD from consanguineous families with apparent phenotypic expansion initially attributed to a single known disease-associated gene were later found to have evidence for MPV.[44]

One subject had a multi-exonic intragenic homozygous *LGI3* deletion confirmed experimentally to be mediated by AAMR, an under-recognized mutational mechanism for SV mutagenesis and generation of pathogenic CNV alleles and exonic deletions.[45] Bi-allelic CNVs are increasingly identified as a cause of autosomal recessive traits (AR-CNV) as a result of their increased detection through bioinformatic tools using ES read-depth analyses.[21,46] Surprisingly, the vast majority (~94%) of AR-CNVs affect a single gene, and more than 75% involve a single or only a few exon(s).[46] Small CNVs, such as the one detected in family 1, often arise *de novo* in a common ancestor and become homozygous alleles via IBD.[47] Similarly, the calculated inbreeding coefficient in family 5A (F = 0.22–0.4) and the overlapping AOH interval of 1.9 Mb in available affected children of family 5 (Figure S2) suggest the private variant in both branches (5A and 5B) is most likely a recent clan/tribal allele that arose in a common distant ancestor at least five generations ago.[47]

In summary, a potentially clinically identifiable genetic PNHS was described in 16 individuals with bi-allelic LoF variants in *LGI3*; the clinical synopsis of the disease trait is characterized by GDD/ID, distal deformities with hyporeflexia/areflexia, involvement of facial musculature in the form of small mouth with restricted opening and facial myokymia, and evidence of motor nerve instability on EMG. Mouse studies revealed that LGI3 is highly expressed at the juxtaparanodal membrane and co-localizes with the voltage-gated potassium channels Kv1.1 and Kv1.2 and associated proteins. Moreover, loss of LGI3 results in reduced and mis-localized Kv1 channel complexes in myelinated axons. Human paralogous gene mutational studies and aggregation of worldwide genomic and molecular data, of multiple variant allele types (SNV and CNV), from eight unrelated families with bi-allelic LoF variants in *LGI3* provide insights into (1) clan genomics and (2) organismal nervous system development and function and (3), with mouse investigations, informs the genesis of electrodiagnostic and clinically observed facial myokymia. Paralogous gene studies may also provide a route to molecular therapies.

Data and code availability

This study did not generate any codes or analyze any datasets. Identified variants have been deposited to ClinVar (ClinVar: SCV002558740 and ClinVar: SCV002558748).

Supplemental information

Supplemental information can be found online at https://doi.org/10.1016/j.ajhg.2022.07.006.

Acknowledgments

We thank the families for their participation in the study. M. Jaegle, A. Aunin, and S. Driegen are thanked for generation of the *Lgi3* knock-out mouse line. This study was supported by the U.S. National Human Genome Research Institute and National Heart, Lung, and Blood Institute to the Baylor-Hopkins Center for Mendelian Genomics (BHCMG, UM1 HG006542), NHGRI Baylor College of Medicine Genomics Research Elucidates Genetics of Rare (BCM-GREGoR; U01 HG011758), U.S. National Institute of Neurological Disorders and Stroke (NINDS) (R35NS105078), National Institute of General Medical Sciences (NIGMS, R01GM 106373), the Muscular Dystrophy Association (MDA; 512848), and Spastic Paraplegia Foundation to J.R.L. D.M. was supported by a Medical Genetics Research Fellowship Program through the United States National Institutes of Health (T32 GM007526-42). J.E.P. was supported by NHGRI K08 HG008986. This study was also supported in part by the JSPS KAKENHI (grant number JP20K07907 to S.M.) and the Japan Agency for Medical Research and Development under grant numbers JP21ek0109486, JP21ek0109549, JP21cm0106503, and JP21ek0109493 to N.M. D.P. is supported by International Rett Syndrome Foundation (IRSF grant #3701-1). D.G.C. is supported by NIH Brain Disorder and Development training grant (T32 NS043124-19) and Muscular Dystrophy Association Development grant (873841). T.F. was funded by Philadelphia University, Amman, Jordan. E.A.F. was funded by King Fahad Medical City Research Centre/IRF 019-052. N.K., S.B., and D. Meijer were supported by the UKRI Biotechnology and Biological Sciences Research Council (BBSRC) grant number BB/N015142/1 (to D. Meijer), grant number BB/T00875X/1 (S.B.), and grant number BB/M010996/1 (N.K.).

Declaration of interests

J.R.L. has stock ownership in 23andMe; is a paid consultant for Regeneron Genetics Center; and is a co-inventor on multiple United States and European patents related to molecular diagnostics for inherited neuropathies, eye diseases, genomic disorders, and bacterial genomic fingerprinting. The Department of Molecular and Human Genetics at Baylor College of Medicine receives revenue from clinical genetic testing conducted at Baylor Genetics (BG); J.R.L. serves on the Scientific Advisory Board (SAB) of BG.

Received: March 27, 2022
Accepted: July 1, 2022
Published: August 9, 2022

Web resources

*AluAlu*CNVPredictor, http://alualucnvpredictor.research.bcm.edu:3838/

ExomeDepth, https://github.com/vplagnol/ExomeDepth

GeneMatcher Browser, https://genematcher.org/

gnomAD Browser, https://gnomad.broadinstitute.org/

NMDEscPredictor, https://nmdprediction.shinyapps.io/nmdescpredictor/

Online Mendelian Inheritance in Man, https://www.omim.org/

SpliceAI, https://spliceailookup.broadinstitute.org/

UCSC Genome Browser, https://genome.ucsc.edu

XHMM, http://atgu.mgh.harvard.edu/xhmm/index.shtml

References

1. Kegel, L., Aunin, E., Meijer, D., and Bermingham, J.R. (2013). LGI proteins in the nervous system. ASN Neuro *5*, 167–181.

2. Staub, E., Pérez-Tur, J., Siebert, R., Nobile, C., Moschonas, N.K., Deloukas, P., and Hinzmann, B. (2002). The novel EPTP repeat defines a superfamily of proteins implicated in epileptic disorders. Trends Biochem. Sci. *27*, 441–444.
3. Herranz-Pérez, V., Olucha-Bordonau, F.E., Morante-Redolat, J.M., and Pérez-Tur, J. (2010). Regional distribution of the leucine-rich glioma inactivated (*LGI*) gene family transcripts in the adult mouse brain. Brain Res. *1307*, 177–194.
4. Bermingham, J.R., Jr., Shearin, H., Pennington, J., O'Moore, J., Jaegle, M., Driegen, S., van Zon, A., Darbas, A., Ozkaynak, E., Ryu, E.J., et al. (2006). The claw paw mutation reveals a role for Lgi4 in peripheral nerve development. Nat. Neurosci. *9*, 76–84.
5. Park, W.J., Lee, S.E., Kwon, N.S., Baek, K.J., Kim, D.S., and Yun, H.Y. (2008). Leucine-rich glioma inactivated 3 associates with syntaxin 1. Neurosci. Lett. *444*, 240–244.
6. Okabayashi, S., and Kimura, N. (2008). Leucine-rich glioma inactivated 3 is involved in amyloid beta peptide uptake by astrocytes and endocytosis itself. Neuroreport *19*, 1175–1179.
7. Lee, S.E., Lee, A.Y., Park, W.J., Jun, D.H., Kwon, N.S., Baek, K.J., et al. (2006). Mouse *Lgi3* gene: expression in brain and promoter analysis. Gene *372*, 8–17.
8. Diehn, M., Sherlock, G., Binkley, G., Jin, H., Matese, J.C., Hernandez-Boussard, T., Rees, C.A., Cherry, J.M., Botstein, D., Brown, P.O., and Alizadeh, A.A. (2003). SOURCE: a unified genomic resource of functional annotations, ontologies, and gene expression data. Nucleic Acids Res. *31*, 219–223.
9. Park, W.J., Lim, Y.Y., Kwon, N.S., Baek, K.J., Kim, D.S., and Yun, H.Y. (2010). Leucine-rich glioma inactivated 3 induces neurite outgrowth through Akt and focal adhesion kinase. Neurochem. Res. *35*, 789–796.
10. Ottman, R., Winawer, M.R., Kalachikov, S., Barker-Cummings, C., Gilliam, T.C., Pedley, T.A., and Hauser, W.A. (2004). *LGI1* mutations in autosomal dominant partial epilepsy with auditory features. Neurology *62*, 1120–1126.
11. Xue, S., Maluenda, J., Marguet, F., Shboul, M., Quevarec, L., Bonnard, C., Ng, A.Y.J., Tohari, S., Tan, T.T., Kong, M.K., et al. (2017). Loss-of-Function mutations in *LGI4*, a secreted ligand involved in schwann cell myelination, are responsible for arthrogryposis multiplex congenita. Am. J. Hum. Genet. *100*, 659–665.
12. Kalachikov, S., Evgrafov, O., Ross, B., Winawer, M., Barker-Cummings, C., Martinelli Boneschi, F., et al. (2002). Mutations in *LGI1* cause autosomal-dominant partial epilepsy with auditory features. Nat. Genet. *30*, 335–341.
13. Morante-Redolat, J.M., Gorostidi-Pagola, A., Piquer-Sirerol, S., Sáenz, A., Poza, J.J., Galán, J., et al. (2002). Mutations in the *LGI1/Epitempin* gene on 10q24 cause autosomal dominant lateral temporal epilepsy. Hum. Mol. Genet. *11*, 1119–1128.
14. Sawlani, K., and Katirji, B. (2017). Peripheral nerve hyperexcitability syndromes. Continuum *23*, 1437–1450.
15. Uy, C.E., Binks, S., and Irani, S.R. (2021). Autoimmune encephalitis: clinical spectrum and management. Pract. Neurol. *21*, 412–423.
16. Chen, Y.Z., Matsushita, M.M., Robertson, P., Rieder, M., Girirajan, S., Antonacci, F., et al. (2012). Autosomal dominant familial dyskinesia and facial myokymia: single exome sequencing identifies a mutation in *adenylyl cyclase 5*. Arch. Neurol. *69*, 630–635.
17. Browne, D.L., Gancher, S.T., Nutt, J.G., Brunt, E.R., Smith, E.A., Kramer, P., and Litt, M. (1994). Episodic ataxia/myokymia syndrome is associated with point mutations in the human potassium channel gene. Nat. Genet. *8*, 136–140.
18. Camelo, C.G., Silva, A.M.S., Moreno, C.A.M., Matsui-Júnior, C., Heise, C.O., Pedroso, J.L., and Zanoteli, E. (2020). Facial myokymia in inherited peripheral nerve hyperexcitability syndrome. Pract. Neurol. *20*, 253–255.
19. Wohler, E., Martin, R., Griffith, S., Rodrigues, E.D.S., Antonescu, C., Posey, J.E., Coban-Akdemir, Z., Jhangiani, S.N., Doheny, K.F., Lupski, J.R., et al. (2021). PhenoDB, GeneMatcher and VariantMatcher, tools for analysis and sharing of sequence data. Orphanet J. Rare Dis. *16*, 365.
20. Froukh, T.J. (2017). Next generation sequencing and genome-wide genotyping identify the genetic causes of intellectual disability in ten consanguineous families from Jordan. Tohoku J. Exp. Med. *243*, 297–309.
21. Plagnol, V., Curtis, J., Epstein, M., Mok, K.Y., Stebbings, E., Grigoriadou, S., Wood, N.W., Hambleton, S., Burns, S.O., Thrasher, A.J., et al. (2012). A robust model for read count data in exome sequencing experiments and implications for copy number variant calling. Bioinformatics *28*, 2747–2754.
22. Jaganathan, K., Kyriazopoulou Panagiotopoulou, S., McRae, J.F., Darbandi, S.F., Knowles, D., Li, Y.I., Kosmicki, J.A., Arbelaez, J., Cui, W., Schwartz, G.B., et al. (2019). Predicting splicing from primary sequence with deep learning. Cell *176*, 535–548.e24.
23. Gonzaga-Jauregui, C., Yesil, G., Nistala, H., Gezdirici, A., Bayram, Y., Nannuru, K.C., Pehlivan, D., Yuan, B., Jimenez, J., Sahin, Y., et al. (2020). Functional biology of the Steel syndrome founder allele and evidence for clan genomics derivation of *COL27A1* pathogenic alleles worldwide. Eur. J. Hum. Genet. *28*, 1243–1264.
24. Ahmed, A., and Simmons, Z. (2015). Isaacs syndrome: a review. Muscle Nerve *52*, 5–12.
25. Kny, E. (1888). Ueber ein dem paramyoclonus multiplex (Friedreich) nahestehendes Krankheitsbild. Archiv f. Psychiatrie *19*, 577–590.
26. Schultze, F. (1895). Beitrage zur Musckelpathologie (Deutsch Ztschr f Nervenh), pp. 65–75.
27. Andermann, F., Cosgrove, J.B.R., Lloyd-Smith, D.L., Gloor, P., and Mcnaughton, F.L. (1961). Facial myokymia in multiple sclerosis. Brain *84*, 31–44.
28. Radü, E.W., Skorpil, V., and Kaeser, H.E. (1975). Facial myokymia. Eur. Neurol. *13*, 499–512.
29. Matthews, W.B. (1966). Facial myokymia. J. Neurol. Neurosurg. Psychiatry *29*, 35–39.
30. Amberger, J.S., Bocchini, C.A., Schiettecatte, F., Scott, A.F., and Hamosh, A. (2015). OMIM.org: online Mendelian Inheritance in Man (OMIM®), an online catalog of human genes and genetic disorders. Nucleic Acids Res. *43*, D789–D798.
31. Satoh, M., Ceribelli, A., and Chan, E.K.L. (2012). Common pathways of autoimmune inflammatory myopathies and genetic neuromuscular disorders. Clin. Rev. Allergy Immunol. *42*, 16–25.
32. Vincent, A., Beeson, D., and Lang, B. (2000). Molecular targets for autoimmune and genetic disorders of neuromuscular transmission. Eur. J. Biochem. *267*, 6717–6728.
33. Irani, S.R., Alexander, S., Waters, P., Kleopa, K.A., Pettingill, P., Zuliani, L., Peles, E., Buckley, C., Lang, B., and Vincent, A. (2010). Antibodies to Kv1 potassium channel-complex proteins leucine-rich, glioma inactivated 1 protein and contactin-associated protein-2 in limbic encephalitis, Morvan's

syndrome and acquired neuromyotonia. Brain *133*, 2734–2748.
34. Kole, M.H., and Cooper, E.C. (2014). Axonal Kv7.2/7.3 channels: caught in the act. Channels *8*, 288–289.
35. D'Adamo, M.C., Liantonio, A., Rolland, J.F., Pessia, M., and Imbrici, P. (2020). Kv1.1 channelopathies: pathophysiological mechanisms and therapeutic approaches. Int. J. Mol. Sci. *21*, E2935.
36. Sonoda, Y., Arimura, K., Kurono, A., Suehara, M., Kameyama, M., Minato, S., Hayashi, A., and Osame, M. (1996). Serum of Isaacs' syndrome suppresses potassium channels in PC-12 cell lines. Muscle Nerve *19*, 1439–1446.
37. Shillito, P., Molenaar, P.C., Vincent, A., Leys, K., Zheng, W., van den Berg, R.J., Plomp, J.J., van Kempen, G.T., Chauplannaz, G., Wintzen, A.R., et al. (1995). Acquired neuromyotonia: evidence for autoantibodies directed against K+ channels of peripheral nerves. Ann. Neurol. *38*, 714–722.
38. Kanaumi, T., Takashima, S., Iwasaki, H., Itoh, M., Mitsudome, A., and Hirose, S. (2008). Developmental changes in *KCNQ2* and *KCNQ3* expression in human brain: possible contribution to the age-dependent etiology of benign familial neonatal convulsions. Brain Dev. *30*, 362–369.
39. Okabayashi, S., and Kimura, N. (2007). Immunohistochemical and biochemical analyses of LGI3 in monkey brain: LGI3 accumulates in aged monkey brains. Cell. Mol. Neurobiol. *27*, 819–830.
40. Ozkaynak, E., Abello, G., Jaegle, M., van Berge, L., Hamer, D., Kegel, L., Driegen, S., Sagane, K., Bermingham, J.R., Jr., and Meijer, D. (2010). Adam22 is a major neuronal receptor for Lgi4-mediated Schwann cell signaling. J. Neurosci. *30*, 3857–3864.
41. Posey, J.E., Harel, T., Liu, P., Rosenfeld, J.A., James, R.A., Coban Akdemir, Z.H., Walkiewicz, M., Bi, W., Xiao, R., Ding, Y., et al. (2017). Resolution of disease phenotypes resulting from multilocus genomic variation. N. Engl. J. Med. *376*, 21–31.
42. Pehlivan, D., Bayram, Y., Gunes, N., Coban Akdemir, Z., Shukla, A., Bierhals, T., Tabakci, B., Sahin, Y., Gezdirici, A., Fatih, J.M., et al. (2019). The genomics of arthrogryposis, a complex trait: candidate genes and further evidence for oligogenic inheritance. Am. J. Hum. Genet. *105*, 132–150.
43. Mitani, T., Isikay, S., Gezdirici, A., Gulec, E.Y., Punetha, J., Fatih, J.M., Herman, I., Tayfun, G.A., Du, H., Calame, D., et al. (2021). Evidence for a higher prevalence of oligogenic inheritance in neurodevelopmental disorders in the Turkish population. Am. J. Hum. Genet. *108*, 1981–2005.
44. Karaca, E., Posey, J.E., Coban Akdemir, Z., Pehlivan, D., Harel, T., Jhangiani, S.N., Bayram, Y., Song, X., Bahrambeigi, V., Yuregir, O.O., et al. (2018). Phenotypic expansion illuminates multilocus pathogenic variation. Genet. Med. *20*, 1528–1537.
45. Song, X., Beck, C.R., Du, R., Campbell, I.M., Coban-Akdemir, Z., Gu, S., Breman, A.M., Stankiewicz, P., Ira, G., Shaw, C.A., and Lupski, J.R. (2018). Predicting human genes susceptible to genomic instability associated with *Alu/Alu*-mediated rearrangements. Genome Res. *28*, 1228–1242.
46. Yuan, B., Wang, L., Liu, P., Shaw, C., Dai, H., Cooper, L., Zhu, W., Anderson, S.A., Meng, L., Wang, X., et al. (2020). CNVs cause autosomal recessive genetic diseases with or without involvement of SNV/indels. Genet. Med. *22*, 1633–1641.
47. Lupski, J.R., Belmont, J.W., Boerwinkle, E., and Gibbs, R.A. (2011). Clan genomics and the complex architecture of human disease. Cell *147*, 32–43.

The American Journal of Human Genetics, Volume *109*

Supplemental information

A reverse genetics and genomics approach to gene paralog function and disease: Myokymia and the juxtaparanode

Dana Marafi, Nina Kozar, Ruizhi Duan, Stephen Bradley, Kenji Yokochi, Fuad Al Mutairi, Nebal Waill Saadi, Sandra Whalen, Theresa Brunet, Urania Kotzaeridou, Daniela Choukair, Boris Keren, Caroline Nava, Mitsuhiro Kato, Hiroshi Arai, Tawfiq Froukh, Eissa Ali Faqeih, Ali M. AlAsmari, Mohammed M. Saleh, Filippo Pinto e Vairo, Pavel N. Pichurin, Eric W. Klee, Christopher T. Schmitz, Christopher M. Grochowski, Tadahiro Mitani, Isabella Herman, Daniel G. Calame, Jawid M. Fatih, Haowei Du, Zeynep Coban-Akdemir, Davut Pehlivan, Shalini N. Jhangiani, Richard A. Gibbs, Satoko Miyatake, Naomichi Matsumoto, Laura J. Wagstaff, Jennifer E. Posey, James R. Lupski, Dies Meijer, and Matias Wagner

SUPPLEMENTAL NOTE: CASE REPORTS

FAMILY 1

Family 1, II-3

The index subject of Family 1 is the second child of consanguineous parents from Pakistan.

His older sister had severe growth delay and was consequently diagnosed with growth hormone (GH) deficiency due to a pathogenic homozygous variant in *GHRHR*. She is successfully treated with GH. In the index subject, global developmental delay as well as growth delay was noted early on, but the boy never had developmental regression. He had muscular hypotonia and poor feeding but never required tube feeding. The same pathogenic variant in *GHRHR* was identified explaining growth delay and GH treatment was initiated at the age of 7 months. He was orthopedically treated for knee contractures for several years. He is currently 8 years old, and his size is 119.2 cm (<1 centile, SDS -2.91), his weight 19.75 kg (<1 centile, SDS -3.07) and his OFC is 49.5cm (<1 centile, SDS-2.72). He has moderate intellectual disability with an IQ of 63 and no signs of autism spectrum disorder. Physical examination revealed short stature, thin build, and both hyper- and hypopigmentations. He had genu valgum, syndactyly, camptodactyly, *pectus excavatum* and spinal kypholordosis. Upon neurological examination, he had no muscle weakness. Deep tendon reflexes could not be provoked and there were no pathologic reflexes. He had mild truncal hypotonia. Myokymia or movement disorder could not be observed. Dysmorphic features included a sandal gap at both feet. He has a triangular face with a pointed chin.

FAMILY 2

Family 2, II-1

The individual is an 11-year-old boy who was referred to Medical Genetics for a history of developmental delays, bilateral hip dysplasia, abnormal electromyogram (EMG) with possible myopathy and mitochondrial cytopathy. He had normal early milestones. He sat unassisted at 6 months of age, was crawling and cruising before the age of one. The delays were noted at around one year of age. He receives speech therapy, occupational therapy, and physical therapy in school. He started to talk at the age of three years. He also has a history of fine motor delays. He has a history of frequent respiratory infections, ER visits and hospitalizations for that. He had an EMG that was an abnormal study with evidence for myokymic discharges creating continuous muscle fiber activity, changes in recruitment of voluntary motor unit activity suggestive of possible myopathy and in addition, bilateral moderately severe median neuropathy at the wrist (carpal tunnel syndrome). He had a muscle biopsy and mitochondrial respiratory chain enzyme analysis which demonstrated increased citrate synthase activity which per lab report was suggestive of mitochondrial proliferation; however, no deficiencies of respiratory chain enzymes were detected before or after correction for increased citrate synthase activity. The family history is notable for a younger brother who is 4 years old and with a history of speech delay and motor delay (he is not walking). The family history is also notable for consanguinity. Parents are first cousins. Neurological assessment depicted: cranial nerves III through XII are intact. His muscle strength in the upper limbs is normal except for mild weakness of the pectoralis major muscles bilaterally, and he has well developed muscles in the upper limbs. In the lower limbs, he has atrophy of the muscles below the knee. He walks with mild flexion of the knees. He is able to stand and take a few steps on his toes, but he is not able to stand or walk on his heels. Perhaps the tibialis anterior

and gastrocnemius muscles are weak. He has -2 hypoactive reflexes symmetrically, and he has bilateral flexor plantar responses. He withdraws to light touch and pinprick, and he also recognizes hot and cold sensations.

Family 2, II-2

The individual is an 8-year-old product of mother's third pregnancy. There were no apparent fetal complications during the gestation, although the mother had achalasia of the cardia and as a result had rather reduced intake and indeed aspirated and experienced pneumonia subsequent to the delivery. This was an unplanned pregnancy. He was delivered by lower segment Cesarean section at term with a birth weight of 7 pounds. He had no perinatal complications including jaundice or respiratory difficulties. Mother became concerned at 1 year when he was not walking. He had x-rays of his hips which were normal and subsequently began physical, occupational, and speech therapy at 15 months of age. Mother notes that he has very good receptive abilities in both English and Arabic which the parents speak at home. He has had no difficulties with his chewing or swallowing. Mother has noticed that he has increasing stiffness over time. He has developed an unusual gait in which he walks with his knees flexed and slightly abducted. He had nerve conduction study (NCS) that showed a slowed peroneal motor conduction velocity with slowed distal latency, low-amplitude tibial motor response with low-amplitude sensory responses. The median palmar latencies were slightly prolonged compared with the ulnar palmar responses. F-waves were within estimate but were poorly formed, but repetitive discharges were noted on F-waves. There was no conduction block or temporal dispersion. Needle examination revealed continuous myokymic-like bursts of motor activity even with deep sedation. No fibrillation potentials or myotonic discharges were noted. There was rapid recruitment of short-duration complex motor unit potentials at most locations with more distal than proximal involvement. The

findings were interpreted as consistent with a neuromyotonic syndrome with myokymic discharges raising the possibility of channelopathy. There were no findings to suggest inflammation, muscle necrosis, vacuolization, or fiber splitting on muscle biopsy. The possibility of very mild median neuropathies at the wrist, right greater than left, was considered, although given the presence of a neuropathy, this interpretation must be made with caution. There has been no history of regression. He also had biopsy of bilateral vastus lateralis muscle and that showed slight denervation atrophy as well as type 1 fiber smallness in some fascicles. At neurological evaluation: His cranial nerves III through XII are intact. His muscle bulk and strength and tone on the upper limbs seem to be age appropriate. However, in the lower limbs, it is not possible to ascertain if his tibialis anterior or gastrocnemius muscles are strong or not, but he has more muscle bulk in those muscles compared to his brother's muscle bulk. Muscle stretch reflexes are -2, symmetric. He has flexor plantar response on the left. His right lower limb was in a cast after surgery for contractures correction. He feels light touch, hot and cold sensations.

FAMILY 3

II-2 and II-3 are the second and third children of healthy, related parents (first cousins), there is a healthy elder brother.

Family 3, II-2

This is a male subject who was 7 years old at last examination. He was born after an uneventful pregnancy, except an elevated risk for Down syndrome on maternal first trimester screening. He was born at full term, birth weight was 3720g, height was 52 cm and OFC was 35 cm. He had global developmental delay, with mild gross motor delay, he started catching objects at 6 months, sitting at 9 months, walking at 18 months, and had difficulties with fine motor skills. Speech was

delayed and he had learning disabilities with special education needs. His feet were normal at birth, then in the first years he was seen for flat valgus feet, that evolved into a bilateral varus deformity needing orthopaedic treatment. He had no seizures. Cerebral and medullar MRI were normal, as well as cardiac and abdominal ultrasound. Hearing and ophthalmological examination were also normal. ENMG was normal. Clinical examination showed normal weight, height and OFC. He had a small mouth with limited opening, a central atrophy of the tongue, and fasciculations of the tongue and of the face, especially around the mouth and eyes. He had talipes equinovarus, and absent deep tendon reflexes on four limbs.

Family 3, II-3

This individual is a female who was 4 years 7 months at last examination. She was born at full term, after an uneventful pregnancy, birth weight was 3560g, length at 51 cm and OFC at 36 cm. She had global developmental delay, held her head at 4 months, and started walking at 18 months. Speech was delayed and she had learning disabilities, but less than her brother. At 18 months, bilateral varus deformity of the feet was noted, and are under orthopaedic treatment. She had no seizures. Cerebral and medullary MRI were normal, as well as cardiac and abdominal ultrasound. Hearing was normal, and she had mild strabismus. EMG showed fasciculations of the muscles of the mouth floor, and absent late F responses. Clinical examination showed normal weight, height and OFC. She had a small mouth with limited opening, a central atrophy of the tongue, and fasciculations of the tongue and of the face, especially around the mouth and eyes. She had talipes equinovarus, more severe than her brother, and absent deep tendon reflexes on four limbs.

FAMILY 4

Case report of this family was previously published (as Family 10 in Froukh 2017).[1]

FAMILY 5

Family 5A, II-1

This is an 11-year-old boy who was referred to genetics clinic along with his sister (Family 5, II-2) with intellectual disability, and FTT. The condition started at age of 2 years with an episode of recurrent abdominal distention and failure to gain weight followed with gastroenterology team and diagnosis of celiac diseases were raised. Later parents noticed some delay in his cognitive skills and speech at 4 years of age. Perinatal history was unremarkable apart from club foot which was corrected surgically at 4 years of age. Parents are not cousins, they have another affected daughter with the same phenotype, and another 5 healthy children. His motor skills were appropriate for age; however, his cognitive and speech millstones were significantly delayed. He can express small sentences which are partially understood by the family, and is able to follow simple commands. Last IQ assessment done was 59. Physical examination unremarkable but the growth parameters for height and weight are below the 3rd centile (130 cm and 26.6 kg). All investigations came negative including, lipid profile, creatine kinase, ammonia, lactic acid, homocysteine, plasma amino acid, urine organic acid, carbohydrate Deficient Transferrin, and acylcarnitine profile. Karyotype revealed normal male 46,XY. Additionally, Electromyography (EMG) and nerve conduction study (NCS) were normal.

Family 5A, II-2

The affected sister is 9 years old with similar presentation of speech delay, intellectual disability and poor school performance. Her physical examination was unremarkable however her growth parameters were below 3rd centile for age (125 cm and 25.5 kg). metabolic and genetic

investigations were unremarkable including normal female 46,XX. Her EMG and NCS are normal, and last IQ assessment was 55.

Family 5B, II-1

This individual is a 13-year-old female with intellectual disability and poor school performance. She also showed delays in her speech, her first word was at age of 3 years. Now she can say few words with poor articulation and with pronunciation difficulties. Physical examination was unremarkable however her growth parameters were below 3rd centile for age. She is wearing eyeglasses for strabismus. Laboratory investigations were unremarkable including normal female 46,XX. MRI brain done and showed normal records. Her last IQ assessment was 69.

Family 5B, II-2

This is a 9-year-old individual who was seen as a case of mild cognitive delay and celiac disease. Family first concern was at the school age. She was found to have learning difficulty when she attended the first grade, she faced significant difficulty in the learning. IQ test was done the result was 66. She was diagnosed to have celiac disease two years back after slow growth. Perinatal history was unremarkable. Her motor development was appropriate for age, although in her cognitive and speech skills delayed. She started to speak at 3 years of age, currently she is at 2nd grade at elementary school. Parents are first cousins, another four daughters and one son. One of the daughters has similar presentation with learning difficulty. Physical examination unremarkable but the growth parameters for height and weight are below the 3rd centile (115 cm and 18.3 kg). All investigations came negative including, lipid profile, creatine kinase, ammonia, lactic acid, homocysteine, plasma amino acid, urine organic acid, and acylcarnitine profile. Karyotype revealed normal female 46,XX. Additionally, array CGH was negative.

FAMILY 6

II-6 (BAB12529), II-1 (BAB12532), and II-5 (BAB12533) are three male siblings born to a consanguineous family from Iraq. They were normal until three to seven months of age when they started showing tremulous movement around mouth and ocular area with posturing and twisting of hands and feet. All three siblings had delayed motor milestones and mild (subjects BAB12529 and BAB12533) to severe cognitive delays (subject BAB12532). Frequent falls and occasional complaints of muscle pain were often observed. Physical examinations revealed facial myokymia in periocular and perioral region in all three siblings. Moreover, finger deformities, inverted posturing of feet, increased tone and reduced deep tendon reflexes (DTR) were consistently present. Their histories and examinations are detailed next.

Family 6, II-1 (BAB12532)

This is the eldest sibling of the three affected males in family 5 and is currently 13 years old. He was born post-term. His history was similar to his siblings, except that his clinical features appeared earlier with onset of occasional tremulous movement around eyes and oral cavity at 3 months of age. He has moderate to severe cognitive impairment and sometimes complains of muscle pain. His family reports continuous improvement in motor skills with age. On examination, he appeared alert and non-dysmorphic. His cranial nerves were intact, and he had normal muscle power. He was hypertonic throughout and had areflexia except for the supinator. He was also noted to have finger deformities/contractures, bilateral varus deformity, inverted posturing of feet. His workup included a normal brain MRI (at 5 years of age) and a normal routine awake and asleep electroencephalogram (EEG) [at 11 years of age].

Family 6, II-5 (BAB12533)

This subject is currently 6 years old. He was born at term and was also developing well until 7 months of age when he gradually developed sudden irritability, posturing/twisting of limbs with tremulous movements. He later showed signs of motor delays and occasional falls and started complaining of muscles pain. Currently, he has mild cognitive impairment, and is partially toilet trained. He can walk independently but with frequent falls. He has exaggeration of ambulation and weakness during febrile illness. He has history of operated diaphragmatic hernia. On examination, he was alert and non-dysmorphic. He had mild abdominal distension. Flickering movement at the perioral area, hypertonia of the limbs, flexion deformities/contractures of fingers, bilateral varus and planter flexion/inversion posturing of feet were also noted. The individual also showed absent DTR except for supinators. His muscle power was 4+/5 throughout. Brain MRI at 5 years of age was normal. NCS of the bilateral median, ulnar, sural, common peroneal and tibial nerves performed at 6 years of age was normal. EMG study however showed evidence of spontaneous activity in the form of fibrillations, positive sharp waves, myokymia, and fasciculations involving multiple cranial, cervical, lumbosacral segments suggestive of an early presentation of motor neuron disease. The CPK level was normal.

Family 6, II-6 (BAB12529)

This subject is currently 3 years old. He was born at term and was developing well until 7 months of age when he gradually developed tremulous movement around mouth and ocular area with posturing and twisting of hands and feet and complaints of muscle pain. His family also reports motor developmental delay (he sat at 18 months of age and walked at 2 years of age). Currently, he has mild cognitive impairment. He walks independently yet falls frequently and runs with difficulty. Additionally, he can go up and down stairs. He often complains of leg pain and weakness, especially in the morning. His family noticed that he becomes weaker and non-

ambulatory during febrile illnesses. On examination, he appeared alert and had no dysmorphic features. He had mild abdominal distension and umbilical hernia. Flexion posturing of fingers and planter flexion and inversion posturing of feet were also noted. He had increased tone throughout and absent DTRs except for left biceps and supinator. He had good muscle power and was able to move all extremities without difficulty.

FAMILY 7

Family 7, II-1

This 16-year-old girl was born to non-consanguineous parents without asphyxia as a first child after an uneventful 39-week gestation. The birth weight, height, and occipito-frontal circumference (OFC) were 3,516 g, 53.0 cm, and 34.0 cm, respectively. Her father felt generalized stiffness at suffering from influenza A. She developed generalized complex partial seizures with or without tonic clonic convulsion from 8 months of age. Interictal EEG was normal. She was diagnosed as epilepsy and took Zonisamide (ZNS). Thereafter, seizures were controlled, and ZNS was stopped at 1y 9m. She was noticed to fist her hands all the time after about 6 months of age. She underwent an operation for umbilical hernia at 1y 1m, and her fisting thereafter exacerbated. She held the head at 3 months, rolled over at 6 months, sat alone at 7 months, crawled at 7 months, creeped at 10 months, stood with support at 10 months, and walked with support at 16 months; she later walked at 34 months with flexed and abducted hips and flexed knees. At 1y 6m, she was neurologically assessed firstly. Her mouth was closed tightly, and her hands were fisted; these were observed to persist during sleep. The hips were flexed and abducted, and knees were flexed. The muscle of the extremities was stiff but is not considered to be spastic by passive stretch. Deep tendon reflexes were not elicited. After 4y 11m, the subcutaneous areas around the corner of the mouth or at the superior eyelid had been observed to twitch; the mother said that a worm moved

here. While she caught a fever from upper respiratory tract infection at 8y 1m, she was motionless with stiffness of the whole body and continued sleeping for four days; the mother said that she was like a stone. While she suffered from varicella at 9y 0m, she was motionless with stiffness for several hours without sleeping. After 11y 10m, she episodically felt vertigo with freezing. Her intellectual development was assessed to be delayed moderately; the intelligence quotient examined by Wechsler Intelligence Scale for Children-Fourth edition at 7y 10m was 41. Electromyography exhibited myokymic discharges at rest. The brain MRI implied mild frontal hypoplasia. Mexiletine was definitely effective, and acetazolamide was in a degree effective for reducing stiffness. Sultiame was effective against episodic vertigo.

FAMILY 8

Family 8, II-2

This 13-year-old male was born spontaneously with no asphyxia as the second child of consanguineous parents whose fathers were brothers. He showed clubfeet and mild contractures in both hands and forearms at birth. His growth and motor development were normal during infancy, but his mother noticed tongue fasciculation and perioral myokymia. Brain MRI and electrophysiological findings (auditory and somatosensory evoked potential and blink reflex) at 6 years of age were unremarkable, when he received orthopedic surgery for clubfeet. At the age of 14 years, he was thin (158.6cm, 46.5kg) and myopathic with thin face, long philtrum and open mouth (Fig. 1P). Tongue fasciculation and perioral myokymia were still present. He could chew and swallow well, but showed dysarthria, such as a conversion of sounds [s], [k] to [t], difficulty in tongue protrusion, and perioral hypersensitivity and extreme contraction around the mouth leading to the difficulty in tooth brushing. Drooling was not apparent, but he slurped saliva frequently. His hip joints were externally rotated, and postoperative *pes planovalgus* was present.

As for upper limbs, only adduction of bilateral thumbs was limited. He could run slowly and could stand over 20 seconds and jump on each leg. He had a severe intellectual disability and was unable to read Hira-kana, which is the simplest form of Japanese letters, but could understand and follow some plain orders and spoke short sentences. He showed hyperactive type of attention-deficit hyperactivity disorder and mild autistic spectrum disorder. He had no seizure episodes ever.

SUPPLEMENTAL FIGURES

Figure S1

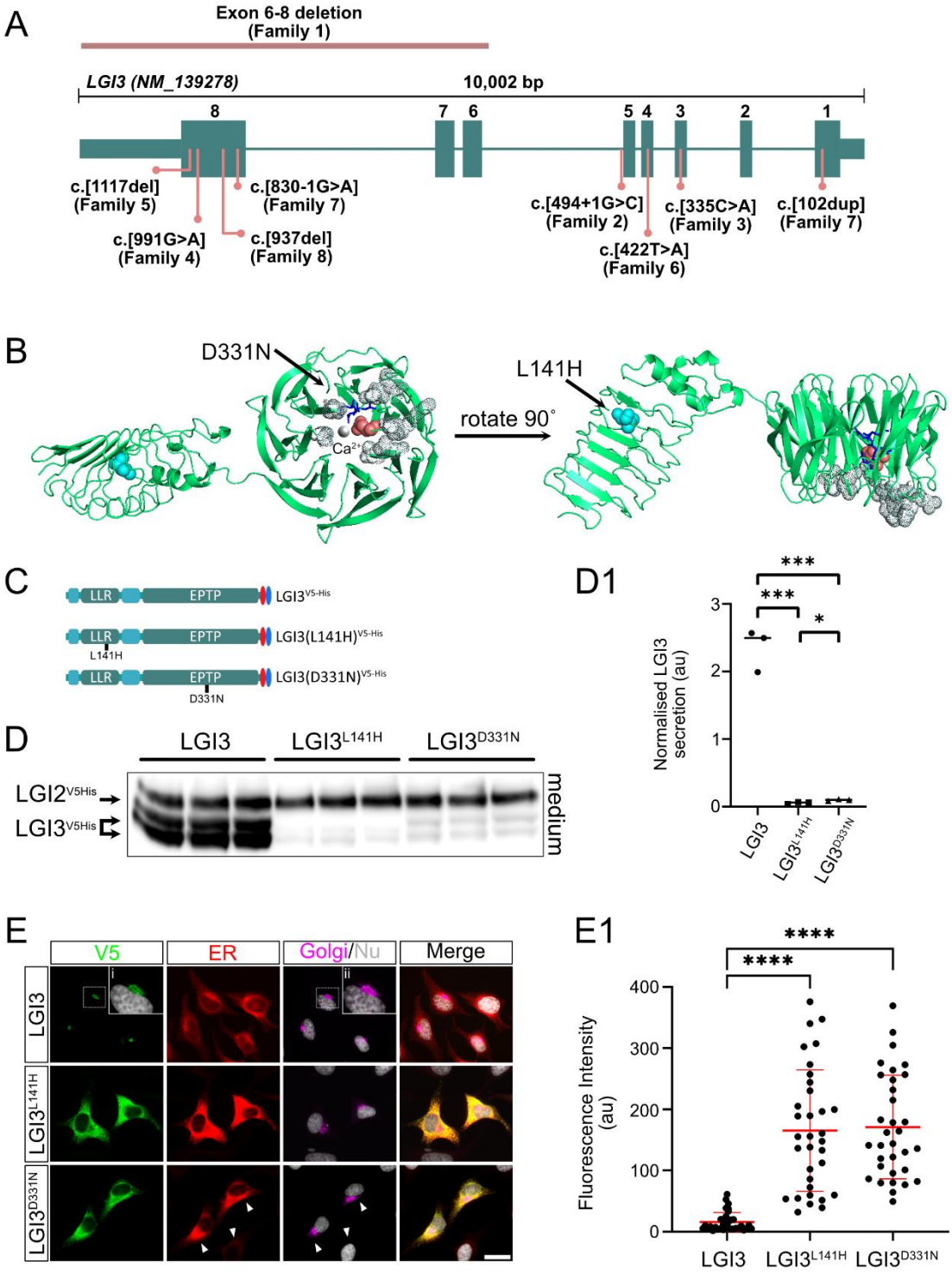

Figure S1. Gene and protein structures of *LGI3* variants and their cell biological expression

(A) Locations and distribution of all identified variants on a liner gene structure of *LGI3* (NM_139278). The green-grey boxes represent exons 1-8 of *LGI3*. The identified variants in this study are marked by red rounded tip arrows.

(B) A structural model of the LGI3 protein was generated using the Phyre2 web application using the structure of LGI1 as a template (PDB file C5Y31B, 53% identity, 100% confidence) and visualized using PyMol.[2; 3] The position of the altered amino acid residues encoded by the two identified missense variants in this study c.422T>A; p.(Leu141His) and c.991G>C; p.(Asp331Asn) are marked by space-filling renditions in light blue and red respectively. The amino acids involved in ADAM22 interactions are indicated with stipled spheres and are located on one side of the EPTP domain. The missense variant L141H is located in the fourth LRR repeat of the LRR domain in a highly conserved patch that is identical in all LGI proteins. The mutation is marked as deleterious by both the PolyPhen2 as well as Phyre2 algorithms. The D331N mutation is located in the hydrophobic core of the EPTP domain and is involved, together with three other negatively charged amino acids (dark blue sticks), in coordinating a Ca2+ ion. The conserved nature of these charged amino acids, present in all LGI proteins, suggest Ca2+ coordination is an important feature of the EPTP domain structure. Indeed, Polyphen2 and Phyre2 mark this mutation as highly unfavourable.

(C) Schematic depiction of expression cassettes of the mouse LGI3 protein and the L141H and D331N LGI33 mutant proteins. The LGI3 proteins carry a V5-tag and 6xHis tag at their carboxy terminal end.

(D) LGI3, $LGI3^{L141H}$ and $LGI3^{D331N}$ proteins were transfected into HEK293T cells, in triplicate, and recovered form tissue culture medium using Ni-NTA agarose affinity precipitation.

Western blotting revealed that whereas LGI3 is readily expressed and secreted, $LGI3^{L141H}$ and $LGI3^{D331N}$ are not. Levels of secretion of the LGI3 proteins were quantified using ImageJ and demonstrated a statistically significant drop in secretion of both mutant proteins. Interestingly, the D332N mutation is less severe, and some secretion of mutant protein is observed. Both mutant proteins still bind to ADAM22 and ADAM23 (not shown).

(E) HEK293T cells were transfected with LGI3, $LGI3^{L141H}$ and $LGI3^{D331N}$ and a Golgi-Scarlet expression cassette. Cells were stained for LGI3 (V5 in green) and the ER (KDEL in red). Purple staining reveals the structure of the Golgi apparatus in transfected cells. Note that the KDEL signal in LGI3 mutant expressing cells is highly increased (white arrowheads point at two transfected cells and one non-transfected cell in the same field of view) suggesting that the mutant proteins elicit a strong ER stress response. LGI3 expression levels (V5 immunefluorescence signal) were quantified, normalized to Scarlet Golgi signal, and plotted in E1. Magnification bar = 15 µm.

Figure S2

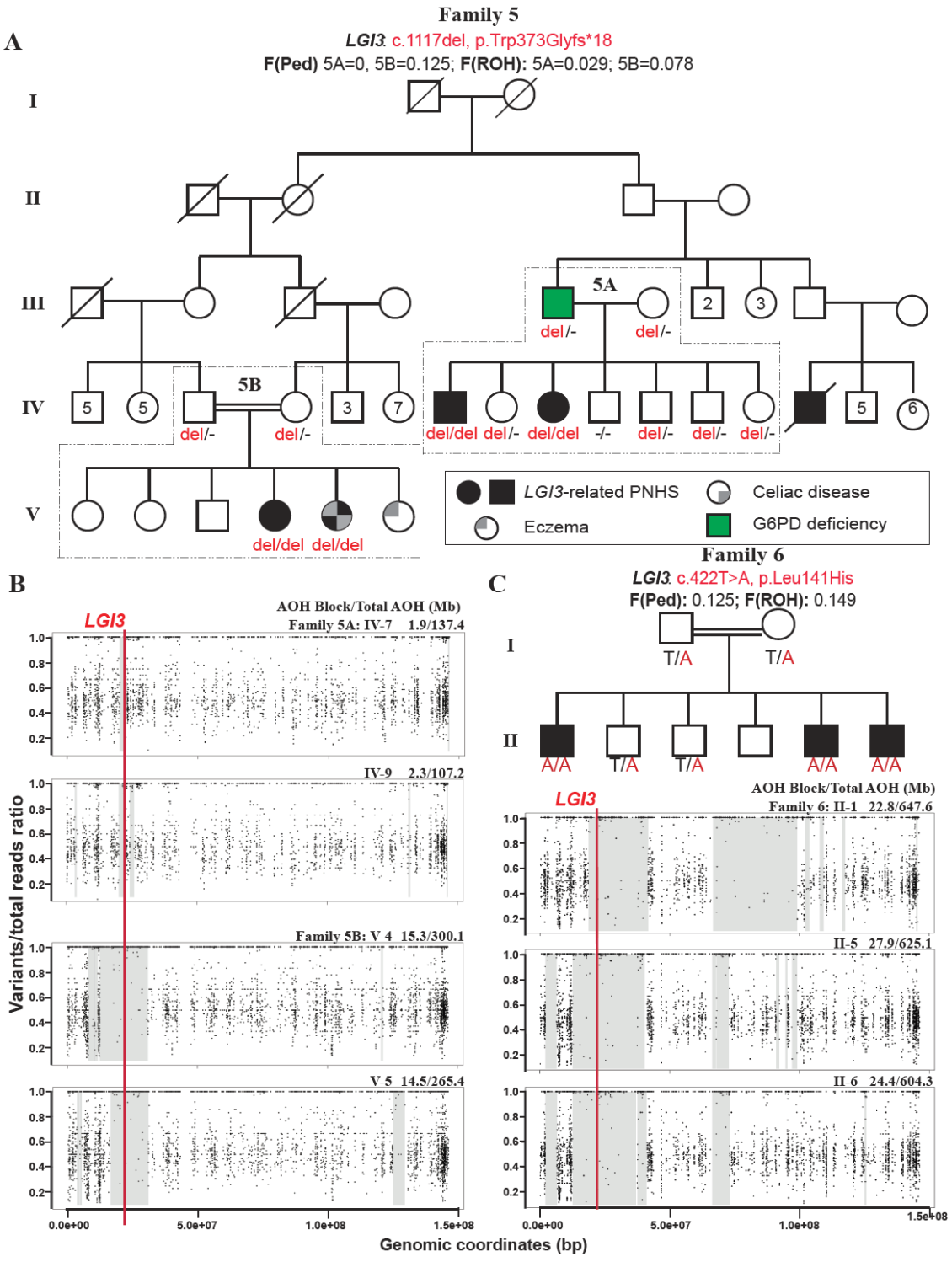
A
Family 5
LGI3: c.1117del, p.Trp373Glyfs*18
F(Ped) 5A=0, 5B=0.125; F(ROH): 5A=0.029; 5B=0.078
I
II
III
IV
V
5A
5B
del/-
del/del
-/-
LGI3-related PNHS
Eczema
Celiac disease
G6PD deficiency
B
LGI3
AOH Block/Total AOH (Mb)
Family 5A: IV-7 1.9/137.4
IV-9 2.3/107.2
Family 5B: V-4 15.3/300.1
V-5 14.5/265.4
Variants/total reads ratio
Genomic coordinates (bp)
C
Family 6
LGI3: c.422T>A, p.Leu141His
F(Ped): 0.125; F(ROH): 0.149
T/A
A/A
Family 6: II-1 22.8/647.6
II-5 27.9/625.1
II-6 24.4/604.3

Figure S2. Extended multigeneration pedigrees of Families 5 and 6 and Absence-of-Heterozygosity (AOH) blocks of affected individuals.

A. The extended multigeneration pedigrees of Family 5 showing both branches of the family (Family 5A and Family 5B). As can also be seen, there is a deceased paternal male cousin of the affected children in Family 5A with a reported phenotype (of global developmental delay, intellectual disability and distal contractures) resembling those of in the spectrum of *LGI3*-related peripheral hyperexcitability syndrome. However, the molecular diagnosis of this deceased cousin could not be confirmed due to unavailability of a biological specimen.

B. Absence of Heterozygosity (AOH) blocks around the *LGI3* variant in the affected individuals from Family 5A and 5B. The position of the *LGI3* variant is marked by a red line. As seen, there is an 1.9 Mb overlapping AOH block denoting a shared haplotype.

C. Pedigree of Family 6 followed by the AOH blocks around the *LGI3* variant in the three affected siblings in the family. The position of the *LGI3* variant is marked by a red line. As seen, the variant falls within a large AOH ranging between 22.8-27.9 Mb.

Figure S3

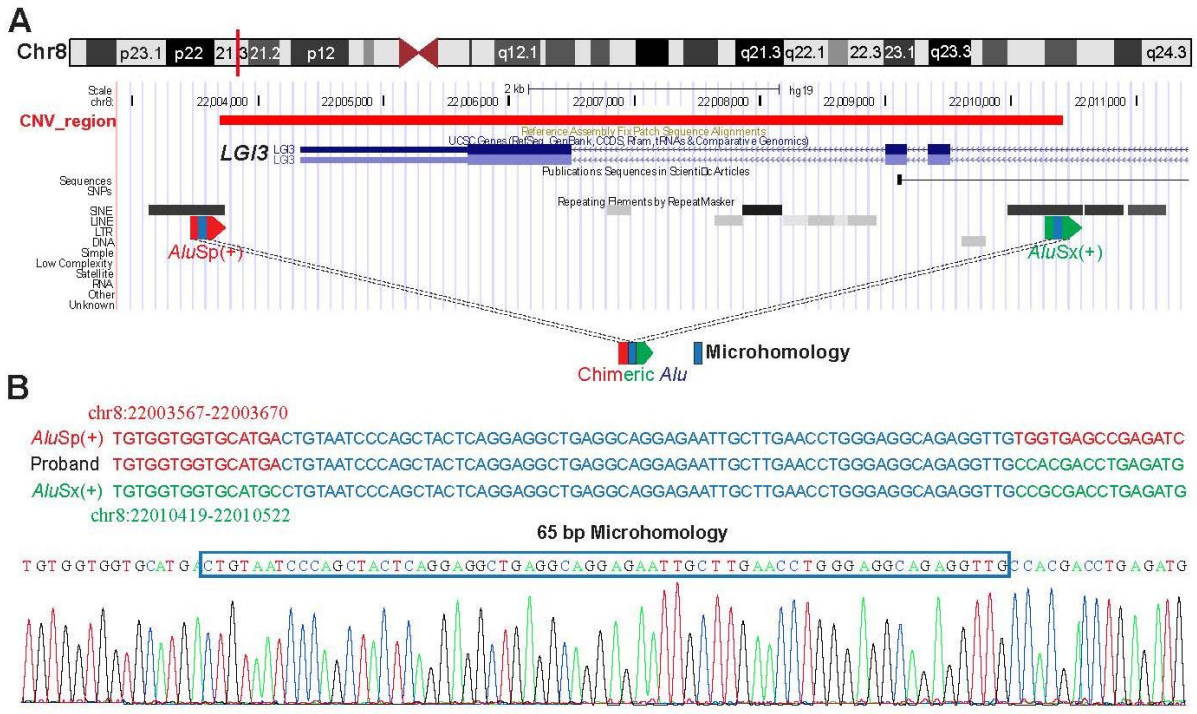

Figure S3. Breakpoint junction analysis of the multi-exonic intragenic deletion of *LGI3* in Family 1 derived from an *Alu/Alu* mediated genomic rearrangement (AAMR)

(A) A genomic view of exons 6 to 8 of *LGI3* from the UCSC genome browser (hg19) shows multiple flanking *Alu* repeats within the targeted genomic interval. The SINE element pair, *Alu*Sp and *Alu*Sx, involved in this AAMR generating the exonic deletion allele are marked with a red and green arrow, respectively, with the microhomology marked in blue. The deletion allele (CNV region) is demarcated by red horizontal bold line.

(B) Breakpoint junction analysis via Sanger sequencing reveals a 6852 bp deletion resulting in a chimeric *Alu* with the breakpoint junction mapping within 65bp microhomology. The three sequences from top to bottom represent the reference *Alu*Sp sequence (colored in red), the sample "chimeric" sequence and the AluSx sequence (colored in green). The region of

microhomology is colored in blue. The bottom image represents Sanger tracing of the breakpoint junction with the 65 bp of microhomology marked with a blue box.

Figure S4

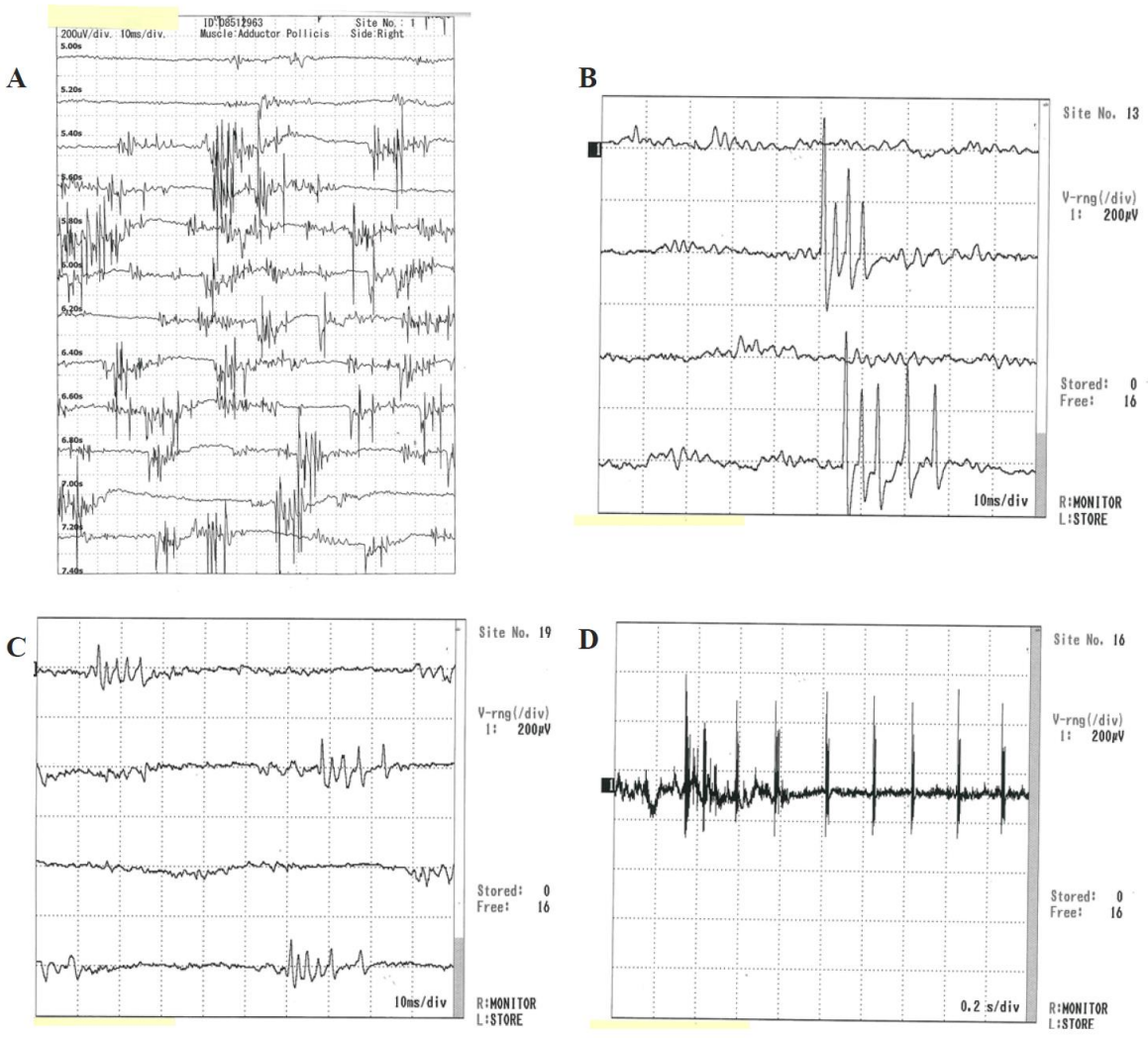

Screenshots of the Electromyogram (EMG) recording of Family 7, II-1.

EMG performed with a concentric needle electrode of right adductus pollicis muscle showing myokymic discharge at rest (Voltage: 200μVol/Division; Sweep speed in Panels A-C is 10ms/division and in Panel D is200ms/division).

Figure S5

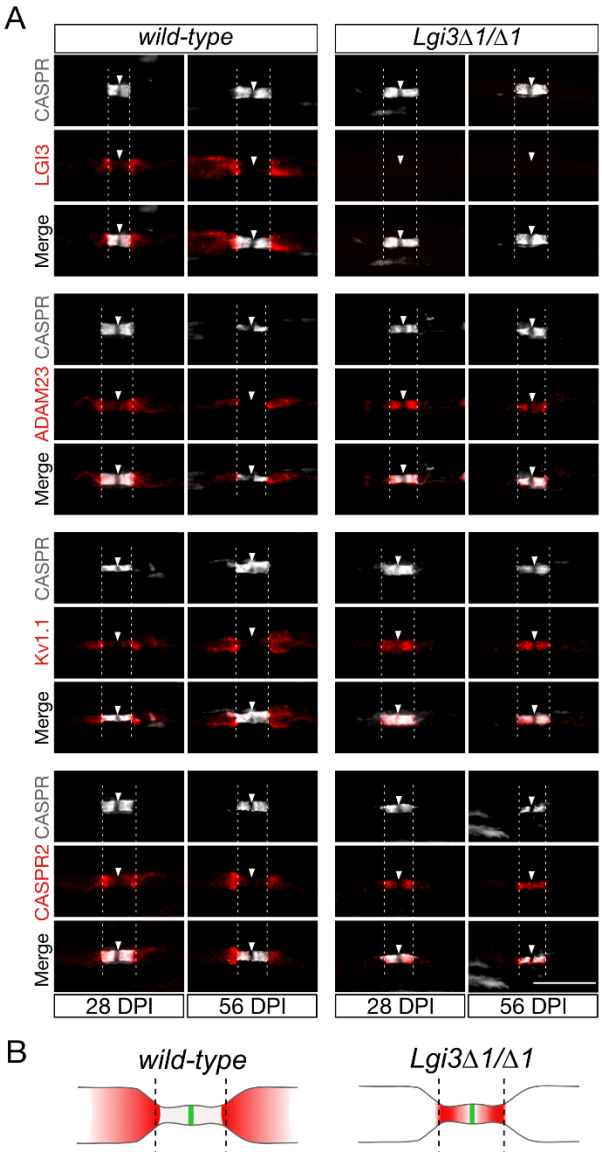

Figure S5 Reassembly of Kv1 channel complexes in remyelinating nerves.

A. Wild-type and *Lgi3*$^{\Delta 1/\Delta 1}$ animals were subjected to crush-injury induced demyelination of the Sciatic nerve. The reassembly of Kv1 channel complexes was examined during remyelination of the injured nerves at 28 and 56 days post injury (DPI) Representative images of the node of Ranvier from immune-stained teased sciatic nerve fibers of wild-

type (left panel) and *Lgi3*$^{\Delta 1/\Delta 1}$ (right panel) mice are shown. Single and merged stains are shown for each image. All images include CASPR (CNTNAP1: in grey) and one of the following: LGI3, ADAM23, Kv1.1 (KCNA1), CASPR2 (CNTNAP2) in red. Scale bar=10µm.

B. Schematic representation of the position of the Kv1 channel complexes (in red) in remyelinated axons (56 DPI) to illustrate the failure to evict the complexes from the paranodal domain in the absence of LGI3. The position of the node is indicated in green.

SUPPLEMENTAL TABLES

Table S1. Other clinical features and investigations in the 16 affected individuals with biallelic deleterious variants in *LGI3*

Family & Individual	Clinical Features					Clinical Investigations				Others
	ASD	**ADHD**	**Abnormal muscle tone**	**Distal deformities**	**Seizures**	**NCS**	**EMG**	**Muscle Biopsy**	**Brain MRI**	
F1, II-3	-	-	+ (calve and truncal hypotonia)	+ (knee contractures)	-	Normal	N/A	N/A	Small hypophysis	Progressive microcephaly (-5 SD); kyphosis; FTT (-4 SD); GH deficiency due to *GHRHR* homozygous pathogenic variant, discrete occasional epileptiform discharge on EEG
F2, II-1	-	-	+ (decreased in LL)	+ (knees, hips, and ankles contractures)	-	N/A	Continuous myokymic discharge, changes in recruitment	Increased citrate synthase activity. No deficiency in RC enzymes	N/A	Bilateral hip dysplasia
II-2	-	-	+ (stiff)	+ (knees, hips, and ankles contractures)	-	Slow CV and prolonged DL (motor peroneal), reduced Amp (tibial); Reduced Amp (tibial), slightly prolonged DL (median palmar compared to ulnar palmar). Poorly formed F-wave with repetitive discharges.	Continuous myokymic discharge. No Fibs or myotonic discharges. Rapid recruitment of short-duration complex MUAP (distal > proximal). Ulnar neuropathy. Median neuropathy at wrist	Slight denervation atrophy; type 1 fiber smallness in some fascicles	N/A	
F3, II-2	+	-	-	+ (talus valgus; bilateral club feet; tapered fingers with	-	N/A	Normal	N/A	Normal	

				spatulated tips)						
II-3	+	-	-	+ (talus valgus; bilateral club feet; mild stiffness of finger joints with no evident camptodactly; adducted thumbs with preserved mobility; mild retraction of toes)	-	N/A	Fasciculations of floor of mouth and absent F response	N/A	Normal	
F4, II-1	+	+	N/A	-	+	N/A	N/A	N/A	N/A	Epileptiform discharge on EEG
II-2	+	-	N/A	-	-	N/A	N/A	N/A	N/A	
F5A, II-1	-	+	-	+	-	Normal	Normal	N/A	N/A	
II-2	-	+	-	+	-	Normal	Normal	N/A	N/A	pectus carinatum
F5B, II-1	-	+	-	+	-	N/A	N/A	N/A	Normal	Anxiety
II-2	-	-	-	+	-	N/A	N/A	N/A	N/A	Celiac disease; Eczema
F6, II-1	-	-	+ (increased)	+ (finger deformities/contractures, bilateral varus deformity, inverted posturing of feet	-	Normal	N/A	N/A	Normal	Frequent falls and occasional muscle pain; normal asleep only EEG
II-5	-	-	+ (increased)	+ flexion deformities/contractures of fingers,	-	Normal	Myokymic discharge, Fibs, PSW, and fasciculations (multiple cranial,	N/A	Normal	Frequent falls and occasional muscle pain; mild abdominal distension and

				bilateral varus and planter flexion/inversion posturing of feet			cervical, and lumbosacral segment)			operated diaphragmatic hernia; normal CPK level
II-6	-	-	+ (increased)	+ (deformities/contractures of fingers, and foot inversion)	-	N/A	N/A	N/A	N/A	Frequent falls and occasional muscle pain; mild abdominal distension and umbilical hernia
F7, II-1	+(Mild)	-	+ (stiff)	+ (flexion and abduction of hips, flexion of knees and fisted hands)	+	Normal	Myokymic discharge at rest	N/A	Suspected mild frontal hypoplasia	Ataxia; Hypokinesia; Operated umbilical hernia; Normal EEG
F8, II-2	-	-	+ (hypotonia)	+	-	N/A	N/A	N/A	Normal	chr16q13.11 microduplication; operated R diaphragmatic hernia
Total	5/16	4/16	7/13	14/16	2/16					

Abbreviations: ADHD, attention deficit hyperactivity disorder; Amp; amplitude; ASD, autism spectrum disorder; CPK, creatine kinase; CV. conduction velocity; Dl, distal latency; EEG, electroencephalography; EMG, electromyography; Fibs, fibrillations; FTT, failure to thrive; GH, Growth hormone; LL. lower limbs; MRI, magnetic resonance imaging; N/A, not available; NCS, nerve conduction study; PSW, positive sharp waves; RS, respiratory chain.

Table S2. Detailed motor and speech developmental milestones in all 16 affected individuals with biallelic *LGI3* variants

Family & Individual	Age at last examination	OFC at birth	Motor development					Speech development			
			Head control	Grabbing	Sitting without support	standing without assistance	Walking without assistance	Babble repetitive syllables (ba. ba. ba)	Says a few words ("mama")	Points to an object or picture	Speaks 50 words and understands more
F1, II-3	7yo	34cm (-1.23 SDS)	N/A	N/A	12 mo	N/A	N/A	19 mo	20 mo	N/A	36 mo
F2, II-1	9yo	N/A	N/A	N/A	6 mo	N/A	4 yo	15 mo	3 yo	N/A	Began more significant vocabulary at age 3y. Started putting three-to-four-word phrases together at 6 y
II-2	6yo	N/A	N/A	N/A	6 mo	N/A	5 yo	N/A	6 yo	N/A	Does not speak, but knows letters, numbers, and colors. He can imitate sounds.
F3, II-1	7yo	35 cm	N/A	6-7 mo	9 mo	N/A	18 mo	N/A	5 yo	N/A	says words but difficult to understand. Comprehends well.
II-2	4yo 7mo	36 cm	4 mo	N/A	11 mo	N/A	18 mo	N/A	N/A	N/A	yes (better than her brother, however, speaks only in her native language not in French)
F4, II-1	22yo	N/A	delayed	N/A	9 mo	delayed	N/A	18 mo	N/A	N/A	6 years with stammer
II-2	20yo	N/A	delayed	N/A	8 mo	delayed	N/A	16 mo	N/A	N/A	N/A

5A, II-1	11yo	N/A	N/A	N/A	N/A	delayed	3 yo	N/A	N/A	N/A	Speaks in sentences with unintelligibility
II-2	9yo	N/A	N/A	N/A	N/A	delayed	2 yo	N/A	N/A	N/A	Speaks in sentences with unintelligibility
F5B, II-1	13yo	N/A	Normal age	N/A	Normal age	Normal age	1 yo	Delayed	Delayed	N/A	She can say 5 words now with poor articulation and difficult pronunciation
II-2	9yo	N/A	Normal age	N/A	Normal age	Normal age	1 yo	3 yo	3 yo	N/A	She can say 3 words sentences with pronunciation problems
F6, II-1	13yo	N/A	2 yo	3 yo	2 yo	2.5 yo	3 yo	2.5 yo	2.7 yo	N/A	4 yo
II-5	6yo	N/A	19 mo	30 mo	30 mo	3 yo	3.5 yo	N/A	2 yo	N/A	started talking in sentences at 5 yo
II-6	3yo	N/A	at expected age	at expected age	18 mo	20 mo	2 yo	> 1 yo	> 1 yo	18 mo	3 yo
F7, II-1	12yo 10mo	34.0cm	3 mo	N/A	7 mo	2yo 6mo	2 yo 10 mo	N/A	2 yo 3 mo	N/A	5yo 2mo
F8, II-2	13yo	34.8cm	4 mo	N/A	N/A	22 mo	22 mo	N/A	N/A	N/A	N/A

Abbreviations: N/A, not available; OFC, Occipitofrontal Circumference; mo, months; yo, years old

SUPPLEMENTAL METHODS

Variant annotation methods and exome sequence analysis

Family 1 - Quad-Exome sequencing of the index case, the unaffected sibling and the parents was performed using a SureSelect Human All Exon 60Mb V6 Kit (Agilent) for enrichment and the NovaSeq6000 (Illumina) platform for sequencing. An average of 135,888,843 reads were produced per sample and aligned to the UCSC human reference assembly (hg19) with BWA v.0.5.8.1 More than 98% of the exome was covered at least 20× and the average depth-of-coverage was more than 126×. Single-nucleotide variants (SNVs) and small insertions and deletions were detected with SAMtools v.0.1.7. Copy number variations (CNVs) were detected with ExomeDepth[4] and Pindel[5]. Variant prioritization was performed based on an autosomal recessive (MAF <0.1%) and autosomal dominant (*de novo* variants, MAF <0.01%) inheritance models.

Family 2- Exome sequencing was performed on genomic DNA extracted from all samples submitted. The exome was captured utilizing the SureSelect Human All Exon V5+UTR kit from Agilent Technologies. Sequencing was performed on an Illumina HiSeq 4000 Paired-end 101 base-pair reads were aligned to a modified human reference genome (GRCh37/hg19) using Novoalign (Novocraft Technologies, Malaysia). Sequencing quality was evaluated using FastQC (www.bioinformatics.babraham.ac.uk/projects/fastqc/). All germline variants were jointly called through GATK Haplotype Caller and followed by PhaseByTransmission to get phasing information.[6] Each variant was annotated using the BioR Toolkit,[7] and subsequently evaluated for clinical relevance by a team of scientists. Genome_GPS v4.0 (formerly named as TREAT)[8] is a comprehensive secondary analysis pipeline for Exome/Whole Genome/Custom Capture sequencing data at Mayo Clinic. FASTQ files were aligned to the hg19 reference genome using

bwa-mem (VN:V7.10) with the default options. Realignment and recalibration was performed using GATK (VN:3.4-46)[6] best practices version 3 for each family separately. Multi-sample Variant calling was performed using the GATK (VN:3.4-46) Haplotype Caller and variants are filtered using variant recalibration Variant Quality Score Recalibrator (VQSR) for both SNVs and INDELs. Identified variants were annotated using BioR[7] framework with functional features, impact prediction, and clinical significance using CAVA, ClinVar, HGMD, and ExAC population frequencies. CNVs are detected using PatternCNV.[9]

Family 3-Exome sequencing was performed on the proband. Genomic DNA was extracted from peripheral blood lymphocytes using a Qiasymphony DNA Midi Kit (Qiagen). A SeqCap EZ MedExome Library kit (NimbleGen, Roche Sequencing) was used for genomic capture. A NextSeq 500 Sequencer was used for massively parallel sequencing. Raw data was analyzed with in-house annotation and analysis pipelines. For data analysis, raw reads were mapped to the human genome reference-build hg19 using the Burrows Wheeler Aligner (BWA MEM v0.717) alignment algorithm (H. Li and Durbin, 2010). The resulting binary alignment/map (BAM) files were further processed by Genome Analysis Tool Kit HaplotypeCaller (GATK HC v3.8) (Van der Auwera et al., 2013). The VCF files are then annotated on Snpeff version 4.3T (Cingolani et al., 2012). The variants are finally identified according to in house criteria. Only coding non synonymous and splicing variants were considered. Variant filtration was conducted according to the transmission mode (*de novo*, autosomal recessive and X-linked), frequency of the variant in the gnomAD database and to our in-house database of n = 866 exomes.

Family 4- Exome sequencing and analysis were performed as previously published in Froukh, 2017.[1]

Family 5- Exome sequencing and analysis were performed as previously published in Bertoli-Avella et al.[10]

Family 6 – Pentad exome sequencing was implemented for the three affected siblings and their parents from Family 6 and was performed at the Human Genome Sequencing Center (HGSC) at Baylor College of Medicine (BCM) through the Baylor-Hopkins Center for Mendelian Genomics (BHCMG) initiative as previously described.[11-13] At HGSC, sequencing was performed using an Illumina dual indexed, paired-end, pre-capture library per manufacturer protocol with modifications as described in the BCM-HGSC protocol (https://www.hgsc.bcm.edu/content/protocols-sequencing-library-construction). Libraries were pooled and hybridized to the HGSC VCRome 2.1[14] plus custom Spike-In design according to the manufacturer's protocol (NimbleGen) with minor revisions. Paired-end sequencing was performed with the Illumina NovaSeq6000 platform with a sequencing yield of 12.2 Gb. Ninety-eight percent of targeted exome bases covered were sequenced to a depth-of-coverge of 20X or greater in all samples. The average depth of coverage for all samples was 119x. Illumina sequence analysis was performed using the HGSC HgV analysis pipeline,[15; 16] which moves data through various analysis tools from initial sequence generation to annotated variant calls (SNPs and intra-read in/dels). In parallel to the exome workflow, a SNP Trace panel was generated for final quality assessment. This included orthogonal confirmation of sample identity and purity using the Error Rate In Sequencing (ERIS) pipeline developed at the HGSC Using an "e-GenoTyping" approach, ERIS screens all sequence reads for exact matches to probe sequences defined by the variant and position of interest. A successfully sequenced sample must meet quality control metrics of ERIS SNP array concordance (>90%). Rare variant family-based exome analysis was performed as previously described.[13] The minor allele frequency of gene variants was obtained from gnomAD[17; 18] and our

in-house generated exome database of ~13,000 individuals at the BCM-HGSC. Variants were confirmed via Sanger sequencing.

Families 7 and 8- Trio exome sequencing was performed on both probands and unaffected parents from Family 7 and proband-only exome sequencing was performed on Family 8 as parental samples were not available. Genomic DNA was captured using the SureSelect Human All Exon V5 kit (Agilent Technologies, Santa Clara, CA, USA) and sequenced on an Illumina HiSeq 2000 or HiSeq 2500 (Illumina, San Diego, CA, USA) with 101-bp paired-end reads.[19] Image analysis and base calling were performed using sequence control software with real-time analysis and CASAVA software (Illumina). Reads were aligned to GRCh37 using Novoalign (http://www.novocraft.com/). Marking of PCR duplicates, indel realignment, and base quality score recalibrations were performed using Picard (http://picard.sourceforge.net/) and Genome Analysis ToolKit (GATK; https://www.broadinstitute.org/gatk/index.php). Variants were called by the GATK UnifiedGenotyper (http://www.broadinstitute.org/gatk/) and annotated using ANNOVAR (http://www.openbioinformatics.org/annovar/) after excluding common variants registered in the common dbSNP135 database (minor allele frequency $\geq$ 0.01). For Family 7, exome mean depth of coverage for the trio was 87.6×, and 95.8% of the total coding sequence of RefSeq genes was covered with a depth of 10× reads or more. For proband from Family 8, exome mean depth of coverage was 56.6×, and 93.8% of the total coding sequence of RefSeq genes was covered with a depth of 10× reads or more.

Family and clan structure and identity-by-descent (IBD)

Absence-of-Heterozygosity (AOH) was calculated in Family 5 and Family 6 from unphased exome data as a surrogate measure of Runs-of-Homozygosity (ROH). This was done using a

bioinformatic tool called BafCalculator (https://github.com/BCM-Lupskilab/BafCalculator) that uses a 1.5 Mb cutoff value to call AOH. We calculated the fraction of the genome covered by ROH region as an estimation of the inbreeding coefficient FROH (Fig. S2). In comparison, the expected coefficient of inbreeding FPED was calculated based on the pedigree structure. The AOH in Family 1 was calculated through an in-house custom made script whereas >7 consecutive homozygous single nucleotide polymorphism (SNPs) are considered an AOH region.[11]

Exonic copy number variant (CNV) and mutational mechanism

To characterize this exonic CNV event, determine breakpoint junctions and infer mutational mechanisms from mutation signatures, long-range PCR was designed with a set of primers flanking the deleted region. AluAluCNVPredictor (http://alualucnvpredictor.research.bcm.edu:3838/), an in-house developed bioinformatic tool to identify the directly oriented CNV-predicted *Alu* pair intersecting the two genomic intervals, was used to further explore the hypothesized mutational mechanism underlying the exonic deletion and examine the AAMR (*Alu*-*Alu* Mediated Rearrangement) genomic instability index for *LGI3*.[20]

Deep clinical characterization

We performed a comprehensive retrospective subjects' medical history and clinical data analysis of the affected subjects including the developmental history, age of onset of disease, growth parameters, central and peripheral neurological features such as tone, reflexes, muscle power, and gait in addition to the presence or absence of abnormal movements such as myokymia and seizures. We also reviewed the findings of the electrodiagnostic and neurophysiological studies including nerve conduction studies (NCS), electromyograms (EMG), electroencephalograms (EEG) in addition to the radiological images, particularly brain Magnetic Resonance Imaging (MRI).

Mouse genetics and Immunohistochemistry

Mice genetics

C57BL6/J mice of both sexes were used in this project. The animals were bred and maintained at the Little France animal unit at the University of Edinburgh, Edinburgh UK. The *Lgi3* $^{\Delta 1/\Delta 1}$ genotype was generated using a standardised gene recombination approach, as previously described.[21] Initially, a LoxP site was inserted upstream of the first exon whilst an Frt-flanked neo cassette with a 3' LoxP site was inserted downstream, resulting in the *Lgi3*^{LoxP} allele.[21] The *Lgi3*$^{\Delta 1}$ null allele was then generated through crossing *Lgi3*$^{LoxP/+}$ mice with mice carrying germline Cre recombinase leading to deletion of the first exon and its promoter (Figure S1). The *Lgi3*$^{\Delta 1/+}$ mice were eventually intercrossed, generating *Lgi3*$^{\Delta 1/\Delta 1}$ offspring. *Lgi3*$^{\Delta 1/\Delta 1}$ mice have a normal life span, are fertile and exhibit no overt abnormal behavior. In line with these findings, another *Lgi3* knock out mouse line analyzed by the International Mouse Phenotyping Consortium (IMPC), confirmed that *Lgi3* null mice are fertile, have a normal lifespan and show no behavioral abnormalities. Genotypes were determined through Polymerase Chain Reaction (PCR) on DNA from ear biopsies. *Lgi3*^{LoxP} and WT alleles were genotyped using primers 5'-GCACGCTGTGTTCCTCAGCTG-3' and 5'-GGGAGAGCAGCCAAAGGATG-3' with expected bands of 302-bp for the WT allele and 344-bp for the floxed allele. The first primer, in combination with primer 5'-GGCAGGAGTCTGGTCCATGC -3' were used for the *Lgi3*$^{\Delta 1}$ allele with expected band of 262-bp for the *Lgi3*$^{\Delta 1}$ allele and 1204-bp for the WT allele. All animal care and procedures were carried out in accordance with the UK Animals (Scientific Procedures) Act 1986 (ASPA).

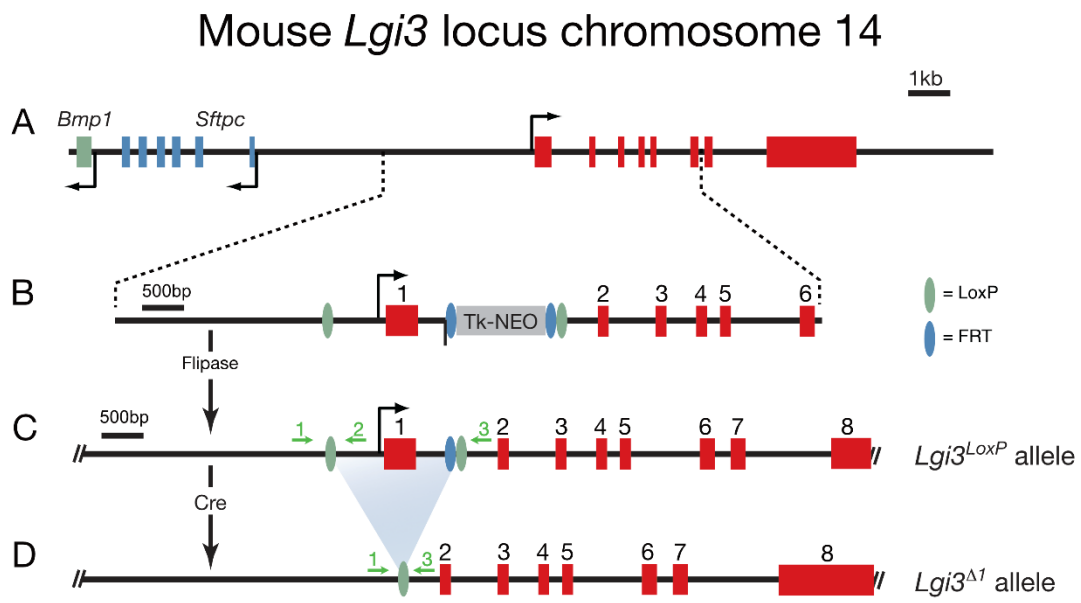

Figure S6: Depiction of the WT mouse *Lgi3* gene locus (mouse chromosome 8) and strategy to generate the $Lgi3^{LoxP}$ and $Lgi3^{\Delta 1}$ alleles.

Sciatic nerve crush

Sciatic nerves crush surgery was performed in 12 weeks old WT *and* $Lgi3^{\Delta 1/\Delta 1}$ mice. All surgical instruments were sterilized by autoclaving before the surgery and again between animals using a bead sterilizer. Following a subcutaneous injection with 10% Vetergesic analgesic diluted in saline (0.01mL per 10g bodyweight), the mouse was placed in an anesthesia chamber filled with 4% isoflurane. The flow was reduced to 2% once full anesthesia was achieved. The mouse was removed from the chamber and the fur was clipped from the operated area. Isoflurane-transferring cone was placed on the animal's nose to ensure continuous anesthesia during the procedure. Body temperature, heart rate and respiration were monitored throughout the operation. The skin was disinfected using iodine-soaked sterile cotton swabs, and surgical drapes were placed around the

incision area. Using dissection spring scissors, a vertical incision was made above the right hip. Once exposed, the sciatic nerve was crushed at the sciatic notch with surgical forceps at three rotation angles, each for 15 seconds. The incision was closed with 2 wound clips per mouse. The animal was transferred to a clean cage placed on top of a heat mat and monitored until conscious. Mice were monitored daily for 72 hours after the procedure; wound clips were removed after 10 days. Mice were culled at appropriate post-surgery time points as described below. Left (control) and right (injured) sciatic nerves were harvested and stored separately prior to processing for immunohistochemistry analysis.

Immunohistochemistry on mouse sciatic nerve

Eight weeks old *Lgi3*$^{\Delta 1/\Delta 1}$ and WT mice were anesthetized using a lethal dose of Sodium Pentobarbital and trans-cardially perfused with 0.1M $NaPO_4$, pH7.4, followed by 4% methanol-free paraformaldehyde (PFA) in 0.1M $NaPO_4$. Sciatic nerves were isolated and post-fixed in 4% PFA solution for 20min. Tissue was then transferred to 0.1M $NaPO_4$ buffer and stored at 4^{o}C until further processing (no longer than 48 hours). To obtain single axon fibres, nerves were initially transferred onto Superfrost Plus™ adhesion microscope slides (ThermoFisher-Scientific) with a large drop of phosphate buffer and cut into shorter fragments. Epineural membrane was removed, and nerve bundles were gently teased apart into single axons using extended acupuncture needles. Teased nerves on slides were air-dried at room temperature (RT) overnight and either used immediately or frozen at -20°C until further use. Before staining, slides with dried or frozen teased nerves were rehydrated with three 5-minute washes in Phosphate Buffered Saline (PBS) followed by a 10-minute incubation in ice-cold 100% Methanol at -20°C. Methanol was washed off with another three 5-minute PBS washes. The slides were transferred into a humidified box and incubated for 1 hour at RT with fish skin gelatin blocking solution (0.3% Triton-X100 in

Sörensen's phosphate buffer, 5% fish skin gelatin - FSG (Sigma-Aldrich)). Primary antibodies were diluted in the same blocking buffer and applied to slides (Table 1.5A). Incubation with primary antibodies was done in a humidified box at 4°C overnight. Slides were then washed six times for 15 minutes at RT with Tris-Buffered Saline (TBS)+ 0.01% Triton-X100. Secondary antibodies (Table 1.5B) were diluted in blocking buffer and incubated on slides for 1 hour in a humidified, light-tight box at RT. This was followed by six 15-minute washes with TBS/0.01%Triton-X 100, one with TBS and one with demi-water. Slides were air-dried in a light-tight box at RT and cover slips were mounted with Mowiol medium. Imaging was done using Zeiss Axio Imager Z1 ApoTome microscope (Carl Zeiss). WT and KO nerve slides were subjected to the same exposure times for reliable analysis. All immunofluorescence images were processed and analysed using Fiji software (ImageJ). Figures were composed using Affinity Designer software.

Table S3

Target	**Isotype**	**Dilution**	**Producer**	**RRID**
CASPR (CNTNAP1)	mouse IgG1	1/200	Lab of Elior Peles	AB_2314220
CASPR (CNTNAP1)	rabbit	1/500	Abcam (ab34151)	AB_869934
Kv1.1 (KCNA1)	rabbit	1/200	Meijer lab UoE	
Kv1.2 (KCNA2)	mouseIgG2b	1/25	Neuromab (K14/16)	AB_2877295
LGI3	rabbit	1/200	Proteintech (21919-1-AP)	AB_10838807
CASPR2 (CNTNAP2)	rabbit	1/500	Genscript (A01426-100)	AB_10838807
PSD95 (DLG4)	mouseIgG2a	1/20	Neuromab (K28/43)	AB_2750659
ADAM23	chicken	1/100	Meijer lab UoE	

Table S4

Source and target	Fluorophore	Dilution	Company	RRID
Goat anti-Mouse IgG1	Alexa488	1/400	ThermoFisher (A21121)	AB_2535764
Donkey anti-Rabbit IgG	Alexa488	1/400	Jackson ImmunoResearch (711-545-152)	AB_2313584
Goat anti-Mouse IgG2a	Alexa555	1/400	ThermoFisher (A21137)	AB_2535776
Goat anti-Mouse IgG2b	Alexa555	1/400	ThermoFisher (A21147)	AB_2535783
Donkey anti-Rabbit	Alexa555	1/400	ThermoFisher (A31572)	AB_162543
Donkey anti-chicken	Alexa647	1/400	Jackson ImmunoResearch (703-605-155)	AB_2340379

Cell culture

HEK293T cells were grown in DMEM supplemented with 10% FBS and 5000 units/ml of Penicillin and Streptomycin at 37˚C in a 5% CO2 incubator. Cells were transfected using PEI-Max or Lipofectamine 3000 following established protocols. Ni-NTA agarose precipitation, Western blotting and quantification was performed as described previously.[22]

SUPPLEMENETAL REFERENCES

1. Froukh, T.J. (2017). Next Generation Sequencing and Genome-Wide Genotyping Identify the Genetic Causes of Intellectual Disability in Ten Consanguineous Families from Jordan. Tohoku J Exp Med 243, 297-309.
2. Kelley, L.A., Mezulis, S., Yates, C.M., Wass, M.N., and Sternberg, M.J. (2015). The Phyre2 web portal for protein modeling, prediction and analysis. Nat Protoc 10, 845-858.
3. Yamagata, A., Miyazaki, Y., Yokoi, N., Shigematsu, H., Sato, Y., Goto-Ito, S., Maeda, A., Goto, T., Sanbo, M., Hirabayashi, M., et al. (2018). Structural basis of epilepsy-related ligand-receptor complex LGI1-ADAM22. Nat Commun 9, 1546.
4. Plagnol, V., Curtis, J., Epstein, M., Mok, K.Y., Stebbings, E., Grigoriadou, S., Wood, N.W., Hambleton, S., Burns, S.O., Thrasher, A.J., et al. (2012). A robust model for read count data in exome sequencing experiments and implications for copy number variant calling. Bioinformatics 28, 2747-2754.
5. Ye, K., Schulz, M.H., Long, Q., Apweiler, R., and Ning, Z. (2009). Pindel: a pattern growth approach to detect break points of large deletions and medium sized insertions from paired-end short reads. Bioinformatics 25, 2865-2871.
6. McKenna, A., Hanna, M., Banks, E., Sivachenko, A., Cibulskis, K., Kernytsky, A., Garimella, K., Altshuler, D., Gabriel, S., Daly, M., et al. (2010). The Genome Analysis Toolkit: a MapReduce framework for analyzing next-generation DNA sequencing data. Genome Res 20, 1297-1303.
7. Kocher, J.P., Quest, D.J., Duffy, P., Meiners, M.A., Moore, R.M., Rider, D., Hossain, A., Hart, S.N., and Dinu, V. (2014). The Biological Reference Repository (BioR): a rapid and flexible system for genomics annotation. Bioinformatics 30, 1920-1922.

8. Asmann, Y.W., Middha, S., Hossain, A., Baheti, S., Li, Y., Chai, H.S., Sun, Z., Duffy, P.H., Hadad, A.A., Nair, A., et al. (2012). TREAT: a bioinformatics tool for variant annotations and visualizations in targeted and exome sequencing data. Bioinformatics 28, 277-278.

9. Wang, C., Evans, J.M., Bhagwate, A.V., Prodduturi, N., Sarangi, V., Middha, M., Sicotte, H., Vedell, P.T., Hart, S.N., Oliver, G.R., et al. (2014). PatternCNV: a versatile tool for detecting copy number changes from exome sequencing data. Bioinformatics 30, 2678-2680.

10. Bertoli-Avella, A.M., Kandaswamy, K.K., Khan, S., Ordonez-Herrera, N., Tripolszki, K., Beetz, C., Rocha, M.E., Urzi, A., Hotakainen, R., Leubauer, A., et al. (2021). Combining exome/genome sequencing with data repository analysis reveals novel gene-disease associations for a wide range of genetic disorders. Genet Med 23, 1551-1568.

11. Karaca, E., Posey, J.E., Coban Akdemir, Z., Pehlivan, D., Harel, T., Jhangiani, S.N., Bayram, Y., Song, X., Bahrambeigi, V., Yuregir, O.O., et al. (2018). Phenotypic expansion illuminates multilocus pathogenic variation. Genet Med 20, 1528-1537.

12. Pehlivan, D., Bayram, Y., Gunes, N., Coban Akdemir, Z., Shukla, A., Bierhals, T., Tabakci, B., Sahin, Y., Gezdirici, A., Fatih, J.M., et al. (2019). The Genomics of Arthrogryposis, a Complex Trait: Candidate Genes and Further Evidence for Oligogenic Inheritance. Am J Hum Genet 105, 132-150.

13. Eldomery, M.K., Coban-Akdemir, Z., Harel, T., Rosenfeld, J.A., Gambin, T., Stray-Pedersen, A., Kury, S., Mercier, S., Lessel, D., Denecke, J., et al. (2017). Lessons learned from additional research analyses of unsolved clinical exome cases. Genome Med 9, 26.

14. Bainbridge, M.N., Wang, M., Wu, Y., Newsham, I., Muzny, D.M., Jefferies, J.L., Albert, T.J., Burgess, D.L., and Gibbs, R.A. (2011). Targeted enrichment beyond the consensus coding DNA sequence exome reveals exons with higher variant densities. Genome Biol 12, R68.

15. Challis, D., Yu, J., Evani, U.S., Jackson, A.R., Paithankar, S., Coarfa, C., Milosavljevic, A., Gibbs, R.A., and Yu, F. (2012). An integrative variant analysis suite for whole exome next-generation sequencing data. BMC Bioinformatics 13, 8.

16. Reid, J.G., Carroll, A., Veeraraghavan, N., Dahdouli, M., Sundquist, A., English, A., Bainbridge, M., White, S., Salerno, W., Buhay, C., et al. (2014). Launching genomics into the cloud: deployment of Mercury, a next generation sequence analysis pipeline. BMC Bioinformatics 15, 30.

17. Collins, R.L., Brand, H., Karczewski, K.J., Zhao, X., Alföldi, J., Francioli, L.C., Khera, A.V., Lowther, C., Gauthier, L.D., Wang, H., et al. (2020). A structural variation reference for medical and population genetics. Nature 581, 444-451.

18. Koch, L. (2020). Exploring human genomic diversity with gnomAD. Nat Rev Genet 21, 448.

19. Sekiguchi, F., Tsurusaki, Y., Okamoto, N., Teik, K.W., Mizuno, S., Suzumura, H., Isidor, B., Ong, W.P., Haniffa, M., White, S.M., et al. (2019). Genetic abnormalities in a large cohort of Coffin-Siris syndrome patients. J Hum Genet 64, 1173-1186.

20. Song, X., Beck, C.R., Du, R., Campbell, I.M., Coban-Akdemir, Z., Gu, S., Breman, A.M., Stankiewicz, P., Ira, G., Shaw, C.A., et al. (2018). Predicting human genes susceptible to genomic instability associated with *Alu*/*Alu*-mediated rearrangements. Genome Res 28, 1228-1242.

21. Jaegle, M., Ghazvini, M., Mandemakers, W., Piirsoo, M., Driegen, S., Levavasseur, F., Raghoenath, S., Grosveld, F., and Meijer, D. (2003). The POU proteins Brn-2 and Oct-6 share important functions in Schwann cell development. Genes Dev 17, 1380-1391.

22. Booth, D.G., Kozar, N., Bradley, S., and Meijer, D. (2021). Characterizing the molecular etiology of arthrogryposis multiplex congenita in patients with *LGI4* mutations. Glia 69, 2605-2617.